UNITED STATES DEPARTMENT OF THE INTERIOR

GEOLOGICAL SURVEY

GEOCHEMICAL RESULTS FROM A NATURAL WATERS STUDY IN THE MOUNT BELKNAP CALDERA AND VICINITY, UTAH

by

Robert E. Tucker, William R. Miller, and

John B. McHugh

Open-File Report 80-1051

1980

Contents

Illustrations

Illustrations--Continued

Tables

Geochemical Results from a Natural Waters Study in the vicinity of the Mount Belknap caldera, Utah

by

Robert E. Tucker, William R. Miller, and

John B. McHugh

ABSTRACT

One hundred and twenty water samples were collected from springs and small unbranched streams in the vicinity of the Mount Belknap caldera, south-central Utah, during the 1979 field season. The water data was evaluated using single-element plots, chemical modeling, and Q-mode factor analysis. The study area has complex geological, geochemical, and mineralogical relationships which are reflected in the chemistry of the waters. Several areas that potentially may contain mineral deposits are described.

ACKNOWLEDGMENTS

J. F. Guadagnoli and J. D. Tucker helped with the sample collection and preparation of samples. D. J. Preston assisted in the chemical analyses and the drafting. Discussions with T. A. Steven, C. G. Cunningham, D. W. Rutherford, G. N. Breit, and J. D. Tucker on the geology and geochemistry of the area, were extremeful helpful.

INTRODUCTION

A geochemical study utilizing samples of water, drainage sediments, and rocks was conducted in the vicinity of the Mount Belknap caldera (fig. 1.). The study a ea is located in the Tushar Mountains, some 20 km (12 miles) northeast of Beaver, Utah, and includes approximately 310 square kilometers (125 square miles). This report of the water geochemistry is one of several pertaining to the geochemistry of the Mount Belknap area.

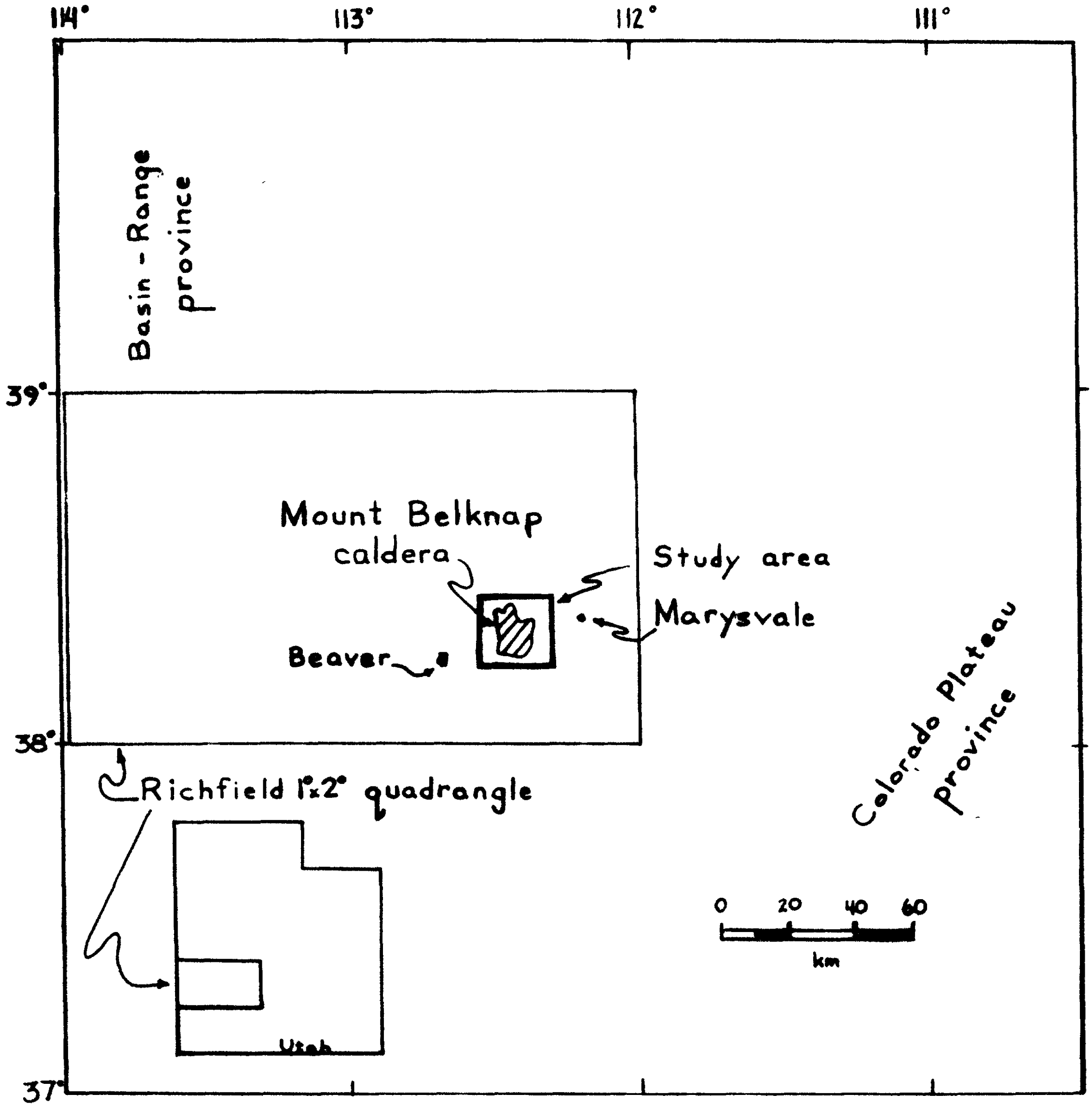

Figure 1

Index map of the Mount Belknap caldera area, Utah.

General geology

The Mount Belknap area is located in the high plateaus section of the Colorado Plateau province near the boundary with the Basin-Range province (fig. 1). The caldera has an area of about 250 square kilometers (75 square miles) and is part of the more extensive Marysvale volcanic field (Cunningham and Steven, 1979b). Paleozoic and Mesozoic limestones and sandstones are exposed east of the Mount Belknap caldera, where they are uncomformably overlain by the extensive Bullion Canyon Volcanics. The Bullion Canyon Volcanics were extruded between 35 and 22 m.y. ago and consist of intermediate-composition lava flows and related volcaniclastic deposits (Steven and others, 1978). These rocks are overlain by the rhyolitic Mount Belknap Volcanics which were extruded between 22 m.y. and 16 m.y. ago (Steven and others, 1978). Basin-Range faulting probably began during eruptions of the Mount Belknap Volcanics (Steven, Cunningham, and Rowley, 1978). The volcanic activity of the area is summarized in table 1. Ages are based on fission-track data for zircon and apatite and K-Ar ages for alunite, natroalunite, biotite, plagioclase and sanidine (Steven, Cunningham, and Rowley, 1978). A generalized geologic map of the Mount Belknap caldera area is given in figure 2. A more complete discussion of the volcanic units in the area is given in Cunningham and Steven, 1978a, 1979b, and 1979d; Steven, 1977; Steven and others, 1978; Steven and Cunningham, 1980a. Gold and base-metal deposits were first discovered in Bullion Canyon in 1868. The Marysvale area has experienced sporadic mining activity since these early discoveries. The mining history is summarized in table 2.

Table 1.--Summary of volcanic activity

35-22 m.y. ago-----	Bullion Canyon Volcanics--latite flows, volcanic breccia, ash-flow tuffs and volcaniclastic deposits.
About 23 m.y. ago--	Quartz monzonite stocks emplaced in Bullion Canyon Volcanics.
22-16 m.y. ago-----	Mount Belknap Volcanics--silicic-alkalic rhyolitic eruptives, flows, ash-flow tuffs, and volcaniclastic deposits.
20 m.y. to present-	Basin-range extensional tectonism and block faulting; some episodic rhyolitic and basaltic volcanism.

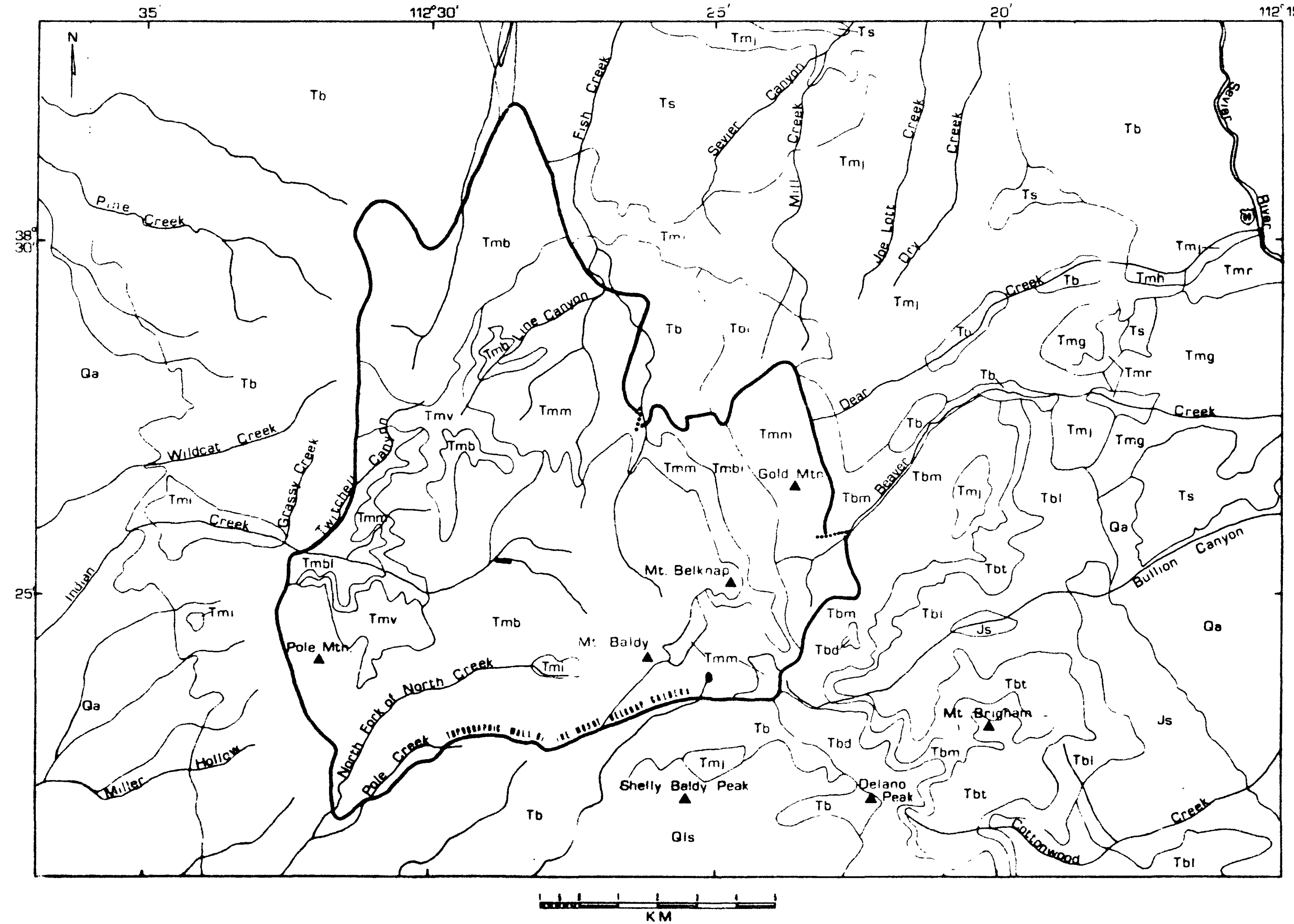

Figure 2 -- Generalized geologic map of the Mount Belknap caldera area, Utah

DESCRIPTION OF MAP UNITS

Qa ALLUVIAL DEPOSITS (HOLOCENE)--Silts, sands, and gravels in alluvial fans, alluvial slope wash, and stream alluvium

Ts SEVIER RIVER FORMATION, LOWER PART (PLIOCENE AND MIOCENE)--Fluviatile gravels, sands, and silts, with interlayered ash-fall tuffs

MOUNT BELKNAP VOLCANICS (MIOCENE)

Tmi Intrusive rocks--Several small porphyritic quartz latitic to rhyolitic stocks containing scattered phenocrysts of quartz, plagioclase, and sanidine in a finely granular mosaic of alkali feldspar and quartz

Tmg Gray Hills Rhyolite Member--Light-gray, spherultically devitrified alkali-rhyolite lava flows containing sparse sanidine phenocrysts. Contorted flow layering is characteristic

Tmr Red Hills Tuff Member--Crystal-poor, welded, white and red alkali-rhyolite ash-flow tuff containing 7-8 percent phenocrysts of anorthoclase, quartz, sodic plagioclase, and minor biotite

Tmj Joe Lott Tuff Member--Crystal-poor welded alkali rhyolite ash-flow tuff containing about 1.5 percent phenocrysts of quartz, plagioclase, and sanidine, with traces of biotite

Tmb Mount Baldy Rhyolite Member--Crystal-poor rhyolite lava flows consisting largely of a fine granular mosaic of quartz and alkali feldspar, and minor plagioclase, biotite, and hematite. Contorted flow layers are common

Tmv Volcaniclastic rocks--Dominantly laharic mud-flow breccias from nearby lava flows of the Mount Baldy Rhyolite Member (Tmb). Some landslide debris and fluviatile sands and gravels are included

Tmm Middle tuff member--Crystal-poor rhyolite welded ash-flow tuff closely similar to that in the outflow Joe Lott Member (Tm)

Tmh Lower heterogeneous member--A sequence of rhyolitic lava domes, lava flows, subordinate ash-flow tuffs, and volcanic sedimentary rocks that lie on or intrude older, intermediate-composition volcanic rocks and are, in part, overlain by the Joe Lott Tuff Member

Tmbl Blue Lake Rhyolite Member--Crystal-poor rhyolite flows closely similar to those in the Mount Baldy Rhyolite Member (Tmb)

BULLION CANYON VOLCANICS (MIOCENE AND OLIGOCENE)

Tbi Intrusive rocks--Strongly porphyritic to equigranular, fine- to medium-grained quartz monzonite containing approximately equal proportions of plagioclase and orthoclase, as much as 20 percent quartz, plus augite, hornblende, and biotite. Minor accessory minerals are apatite, zircon, and Fe-Ti oxides

Tb Heterogeneous lava flows and volcanic breccias--Range from thick porphyritic rhyodacite and quartz latite flows containing phenocrysts of plagioclase, biotite, and clinopyroxene, to fine-grained dark lava flows and breccias of intermediate composition, with small phenocrysts of plagioclase and clinopyroxene

Tbd Delano Peak Tuff Member--Densely welded crystal-rich quartz latite ash-flow tuff containing phenocrysts of plagioclase (32 percent), hornblende (9 percent), Fe-Ti oxide minerals (4 percent), and less than 1 percent each of quartz, biotite, and apatite

Tbm Middle member--Mostly light-gray and brown rhyodacite lava flows, flow breccia, and volcanic mud-flow breccia that lie between the overlying Delano Peak Tuff Member (Tbd) and underlying Three Creeks Tuff Member (Tbt)

Tbt Three Creeks Tuff Member (Oligocene)--Densely welded light-gray and brown, crystal-rich quartz latite ash-flow tuff containing phenocrysts of plagioclase (35 percent), hornblende (9 percent), biotite (3 percent), and quartz (2 percent). Fe-Ti oxide minerals, sanidine, and other accessory minerals occur in traces. K-Ar age is 27 m.y. (Steven and others, 1979)

Tbl Lower member--Mostly volcanic mudflow breccia, flow breccia, and tuffaceous sedimentary rocks that occur below the Three Creeks Tuff Member (Tbt)

COMPOSITE OF SEDIMENTS (JURASSIC, TRIASSIC, AND PERMIAN)

Js Sedimentary rocks--Includes the Arapien Formation, the Navajo Sandstone, Chinle Formation, Shinarump Formation, Moenkopi Formation, Kaibab Limestone, Toroweap Formation and the Queantoweap Sandstone of McNair (1951)

CORRELATION OF MAP UNITS

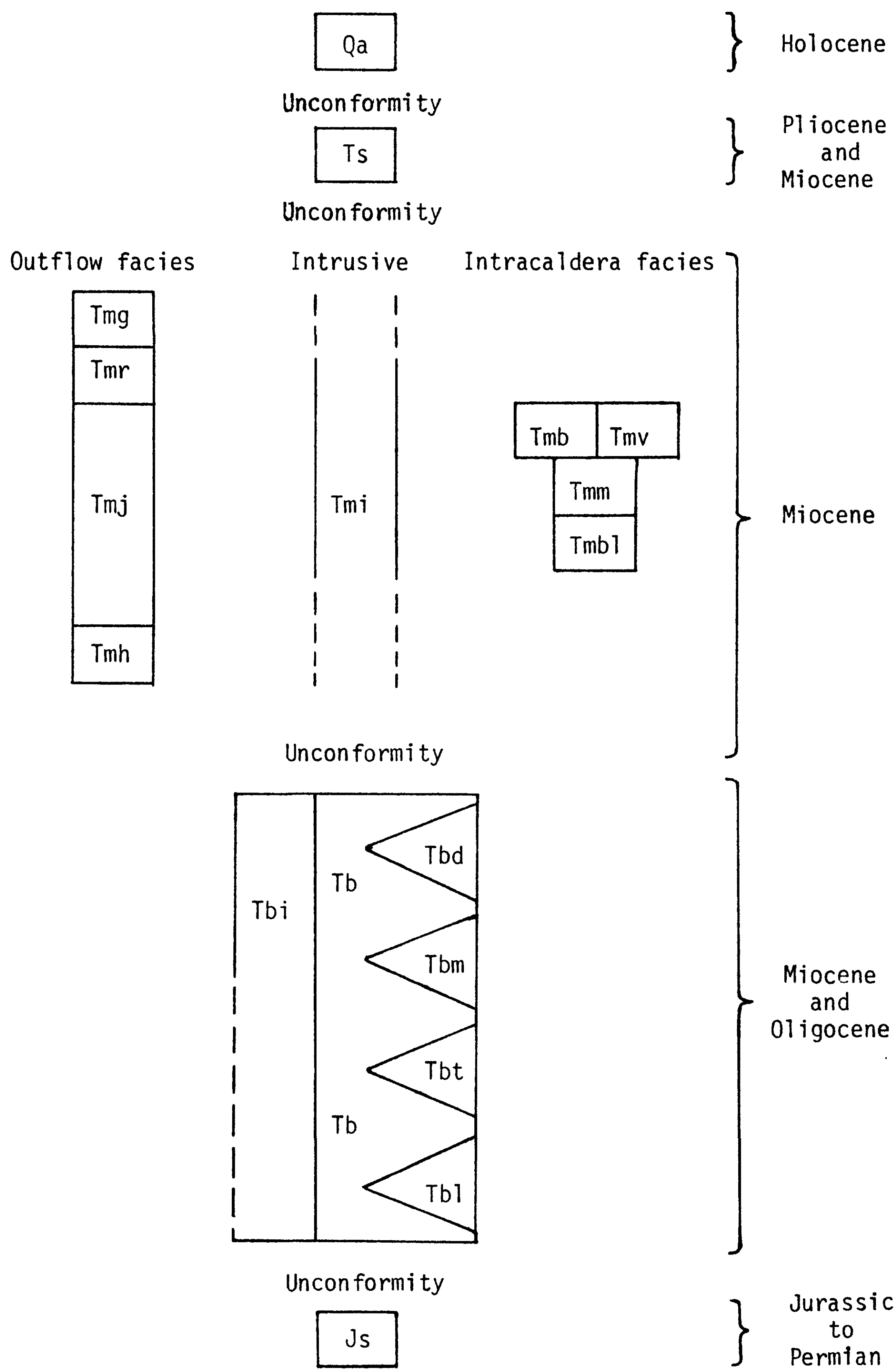

Table 2.--Mining history

Year	History
1868	Precious and base-metal discoveries in Bullion Canyon. Manto deposits in Mesozoic sediments.
1890	Small gold and silver deposits discovered throughout Tushar Mountains.
1900	Kimberly deposits developed, richest precious metal deposits in the region.
1910	Alunite discovered, mined for potash during World War I, and aluminum during World War II.
1949	Uranium discovered in vein deposits north of Marysvale.
1980	No active mining in the region, however, exploration for uranium, precious and base metals is being actively pursued.

SAMPLE COLLECTION AND ANALYTICAL PROCEDURES

Water samples were collected from 39 springs and 77 small unbranched streams. Samples 7937 and 7939, 7987 and 7988, 7993 and 7994, 8008 and 8009 are site duplicates. Samples 7941 and 7942 were collected from main tributary streams (fig. 3). The techniques for water sample collection are described in Miller and others (1980). The analytical method used to determine each constituent is listed in table 3. It should be noted that, except for the few samples collected in the Kimberly and Bullion Canyon areas, the waters probably are not contaminated by mining or cultural activity.

GEOCHEMISTRY OF THE WATERS

Water geochemistry can be useful as an exploration media and in gaining an understanding of the geological and geochemical processes occurring in an area. Background information and limitations of applying hydrogeochemical surveys to exploration can be found in Boyle and others (1971), Cameron (1978), and Miller and others (1979, 1980).

A summary of the chemical analyses is given in table 4. High values for sodium, potassium, magnesium, calcium, barium, boron, lithium, chloride, and sulfate are concentrated in the Kimberly area, Mill Creek, and along the western margin of the caldera (figs. 4-12). Values for silica, iron, and aluminum are slightly anomalous along the western margin but are moderately anomalous along a linear feature extending from Twitchell Canyon through Line Canyon (figs. 13-15). There are anomalous values within the caldera, also.

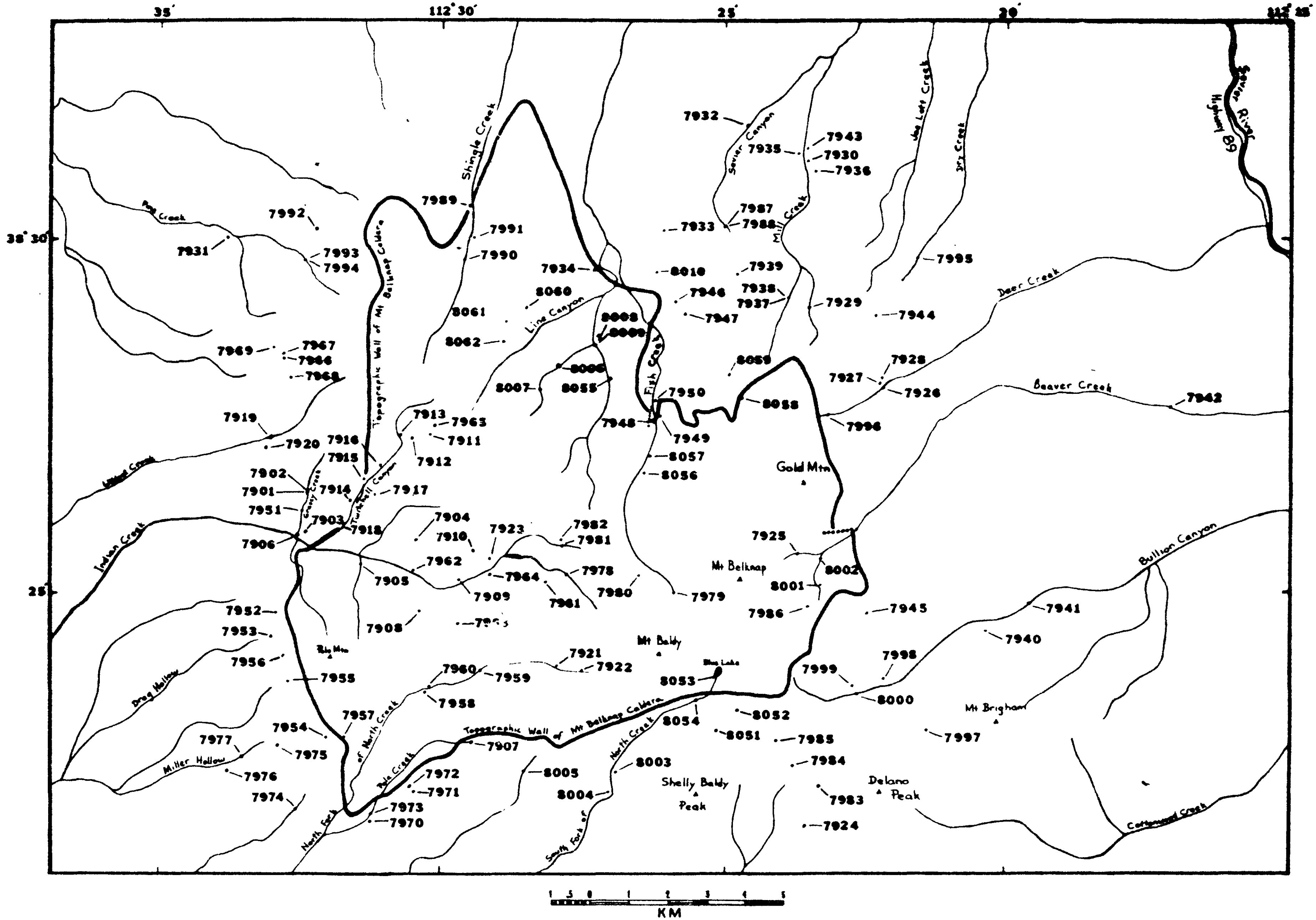

Figure 3 Sample sites, Mount Belknap caldera area, Utah

Table 3.--Analytical methods used for water analyses, Mt. Belknap Caldera, Utah

Constituent	Method	Reference
Alkalinity	Gran's plot potentiometric titration	Orion Research, Inc. (1975).
Sulfate	Ion chromatography	Smee and Hall (1978).
Chloride	---do	Do.
Fluoride	---do	Do.
Calcium	Flame atomic absorption spectrophotometry	Perkin-Elmer Corp. (1976).
Magnesium	---do	Do.
Sodium	---do	Do.
Potassium	---do	Do.
Lithium	---do	Do.
Silica	---do	Do.
Zinc	---do	Do.
Copper	Flameless atomic absorption spectrophotometry	Perkin Elmer Corp. (1977).
Molybdenum	---do	Do.
Lead	---do	Do.
Arsenic	---do	Do.
Iron	---do	Do.
Strontium	Induction-coupled-plasma-atomic-emission-spectrometry (ICP)	No reference
Barium	---do	Do.
Boron	---do	Do.
Beryllium	---do	Do.
Manganese	---do	Do.
Aluminum	---do	Do.
Uranium	Fluorometric	McHugh (1979).
Specific conductance	Conductivity bridge	Brown, Skougstad, and Fishman (1970)

Table 4.--Summary of chemical analyses of 122 water samples, Mount Belknap caldera, Utah

Constituent	Minimum	Maximum	Mean	Geometric mean	Standard deviation	Geometric deviation
Ca (mg/L)	1.3	130.	23.7	13.3	28.1	2.90
Mg (mg/L)	0.20	71.	5.70	2.45	10.6	3.27
Na (mg/L)	0.92	57.	8.20	5.63	9.03	2.28
K (mg/L)	0.04	5.3	1.09	0.803	0.961	2.24
Li (µg /L)	1.0	70.	4.83	2.45	9.20	2.77
Sr (µg/L)	5.0	2100.	215.	82.4	363.	3.98
Ba (µg/L)	0.50	178.	19.1	5.42	32.2	5.39
B (µg/L)	3.0	56.	7.19	4.53	9.36	2.27
Be (µg/L)	0.10	26.	0.734	0.215	2.57	3.48
SiO_2 (mg/L)	2.1	63.	20.3	17.6	10.2	1.80
Alkalinity (mg/L)	0.01	361.	60.5	15.5	74.7	17.1
SO_4 (mg/L)	0.47	364.	20.0	7.58	42.8	3.52
Cl (mg/L)	0.15	205.	9.41	3.59	21.2	3.83
F (mg/L)	0.04	27.	0.676	0.300	2.47	2.74
Zn (µg/L)	1.0	290.	9.89	4.86	30.7	2.38
Cu (µg/L)	0.10	9.2	1.33	0.809	1.39	2.85
Mo (µg/L)	0.30	6.8	0.654	0.565	0.635	1.57
Pb (µg/L)	0.10	5.8	0.807	0.577	0.774	2.34
As (µg/L)	1.1	11.	2.73	2.48	1.39	1.51
Fe (µg/L)	0.50	740.	38.8	16.7	75.8	3.72
Mn (µg/L)	1.0	2270.	47.6	2.70	269.	5.14
Al (µg/L)	25.	14280.	228.	74.6	1291.	2.76
U (µg/L)	0.10	490.	6.67	0.513	47.7	4.19
Sp. Cond. (µmhos/cm)	15.	1050.	201.	129.	212.	2.51
pH	4.4	8.55	7.58	--	0.619	--
Temp (°C)	2.0	23.	9.21	8.34	4.12	1.58

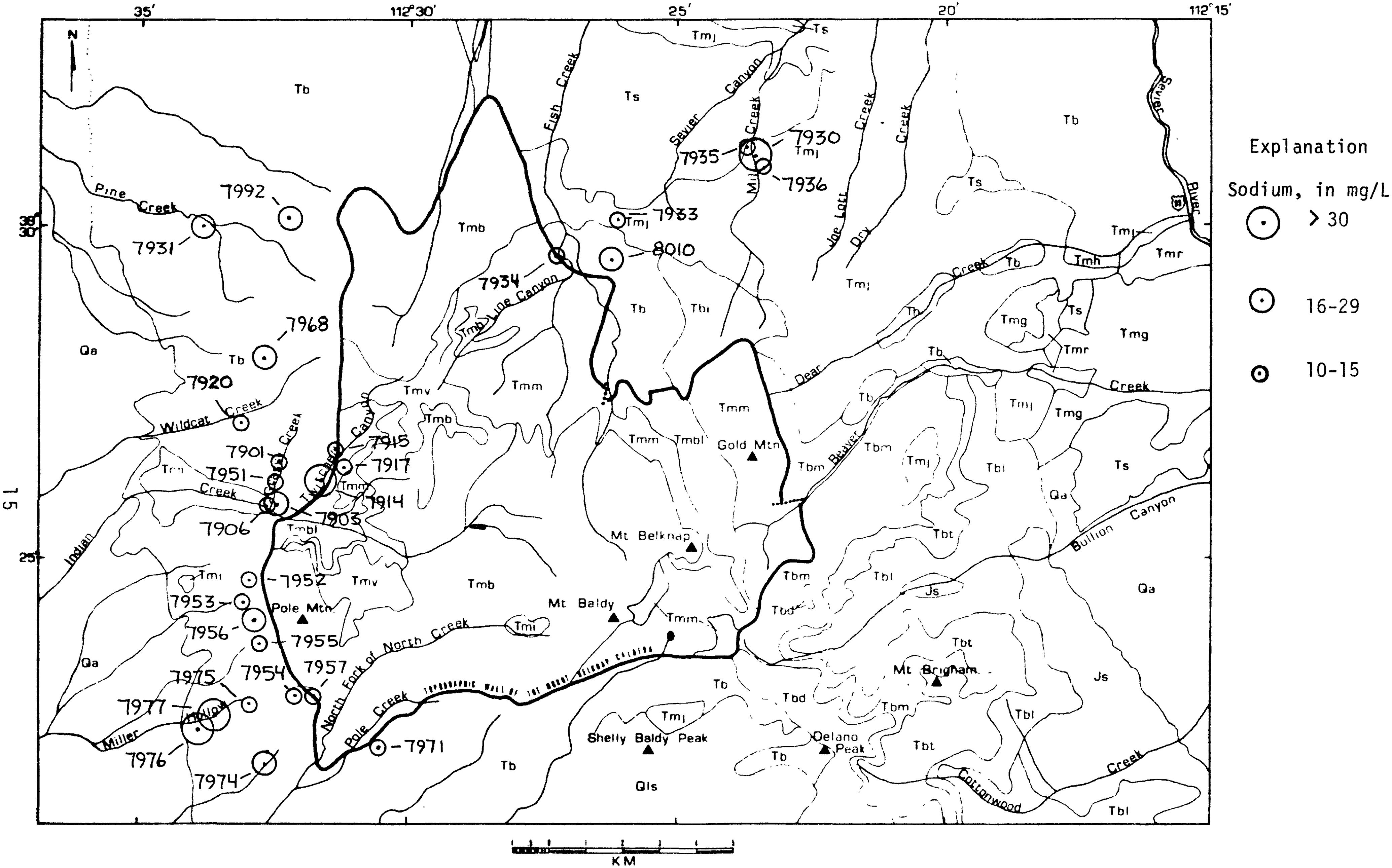

Figure 4 -- Distribution of anomalous sodium concentrations in the Mount Belknap caldera area, Utah. Numbers are those of sample sites. See figure 2 for description of geologic units.

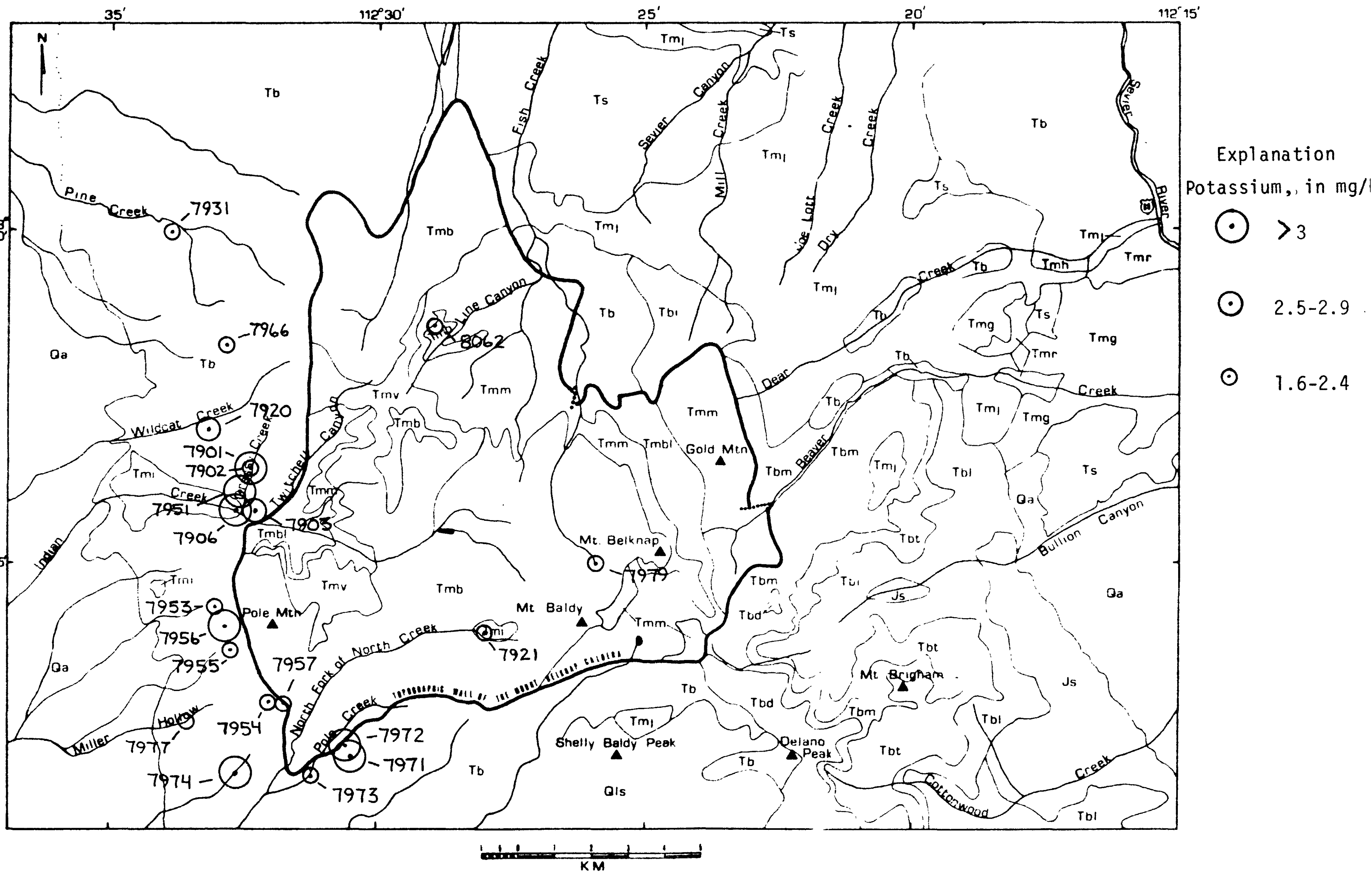

Figure 5 -- Distribution of anomalous potassium concentrations in the Mount Belknap caldera area, Utah. Numbers are those of sample sites. See figure 2 for description of geologic units.

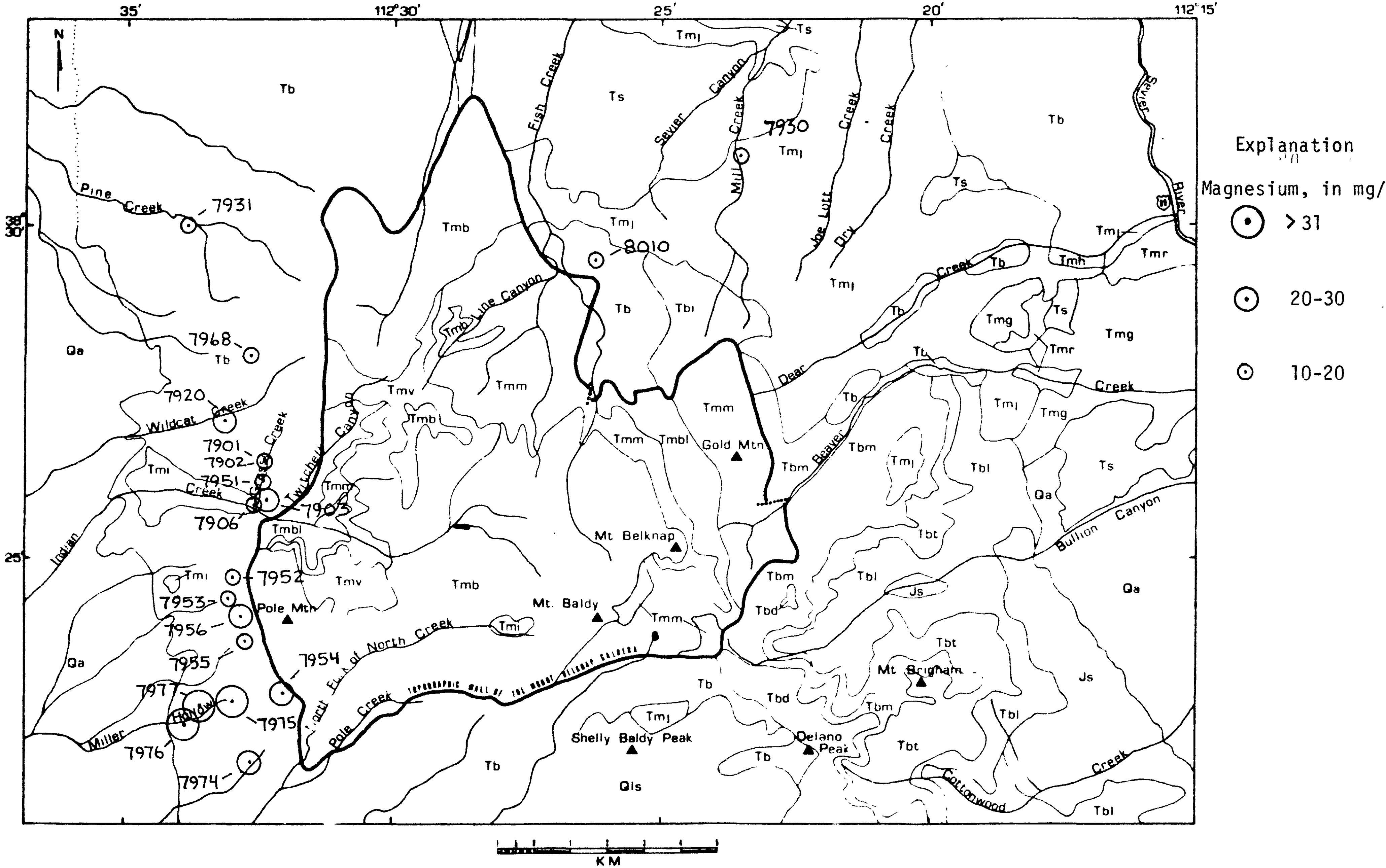

Figure 6 -- Distribution of anomalous magnesium concentrations in the Mount Belknap caldera area, Utah. Numbers are those of sample sites. See figure 2 for description of geologic units.

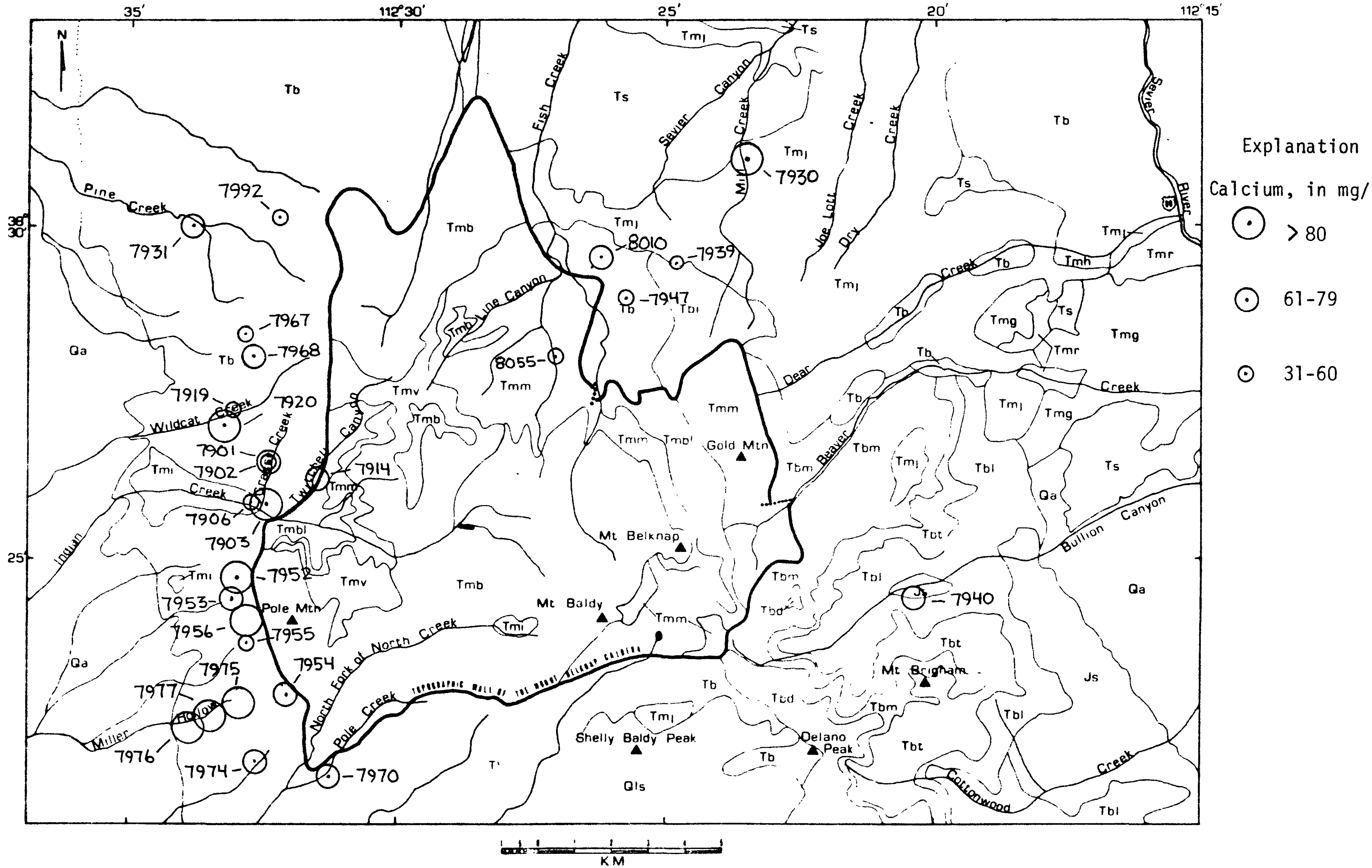

Figure 7 -- Distribution of anomalous calcium concentrations in the Mount Belknap caldera area , Utah. Numbers are those of sample sites. See figure 2 for description of geologic units.

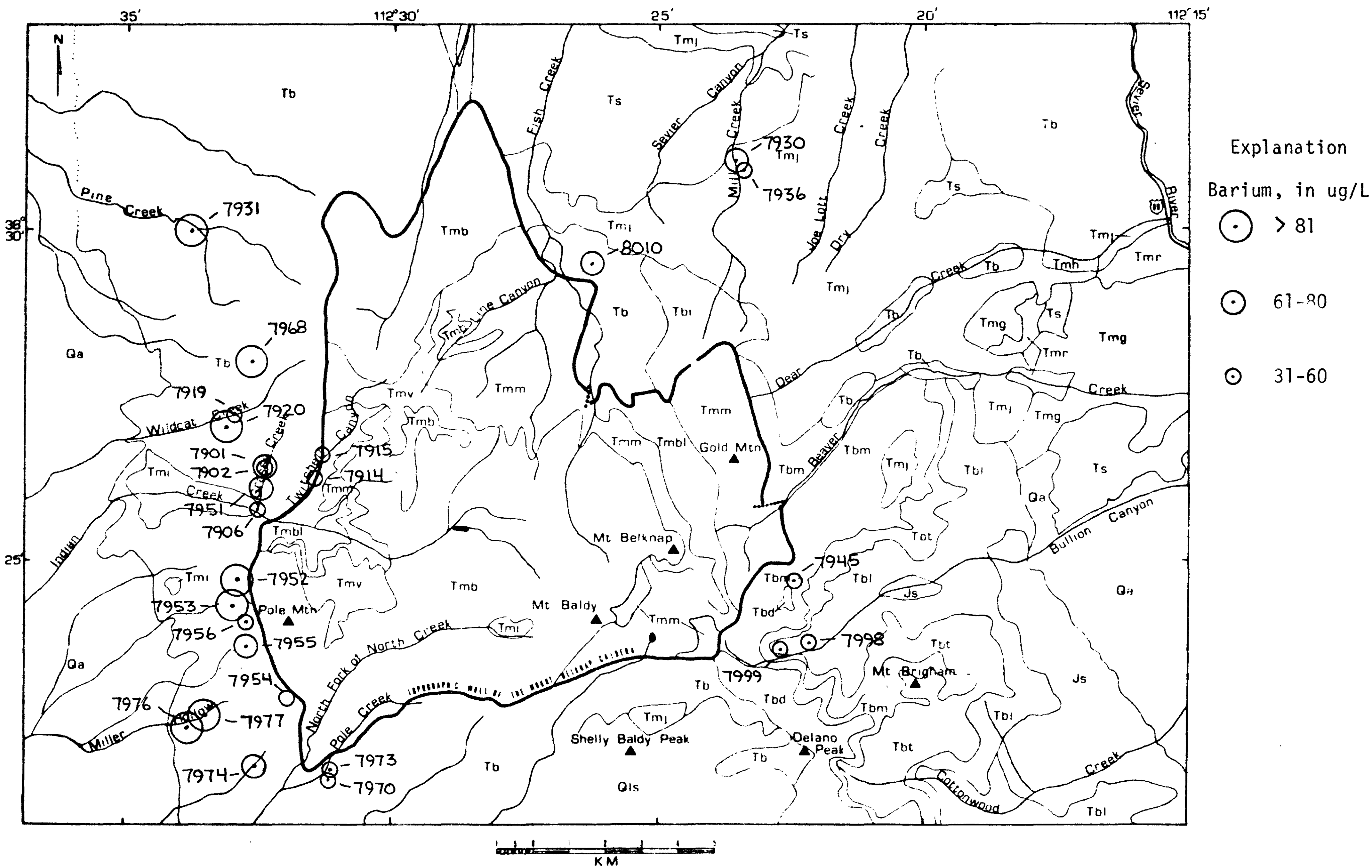

Figure 8 -- Distribution of anomalous barium concentrations in the Mount Belknap caldera area, Utah. Numbers are those of sample sites. See figure 2 for description of geologic units.

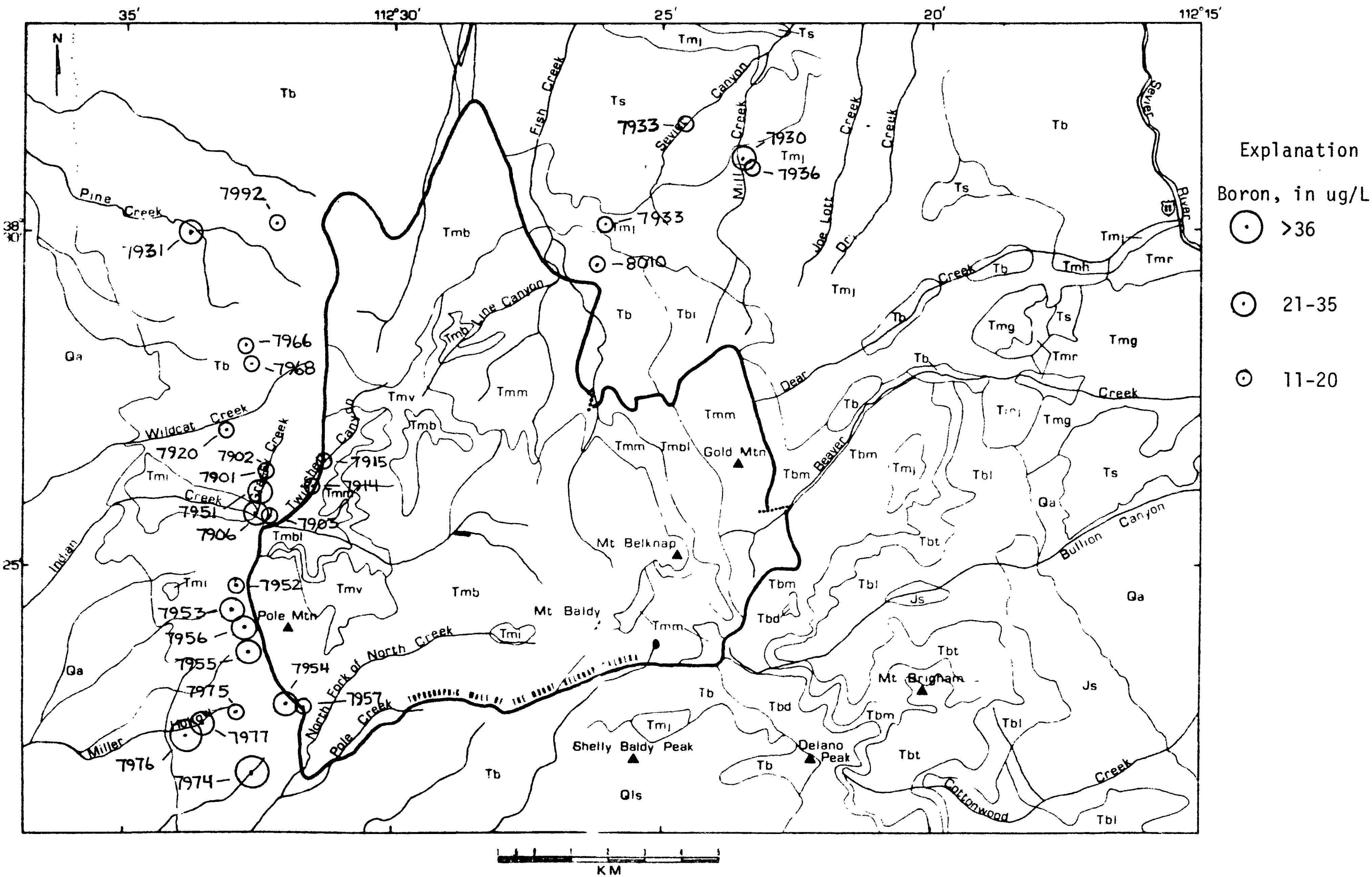

Figure 9 -- Distribution of anomalous boron concentrations in the Mount Belknap caldera area, Utah. Numbers are those of sample sites. See figure 2 for description of geologic units.

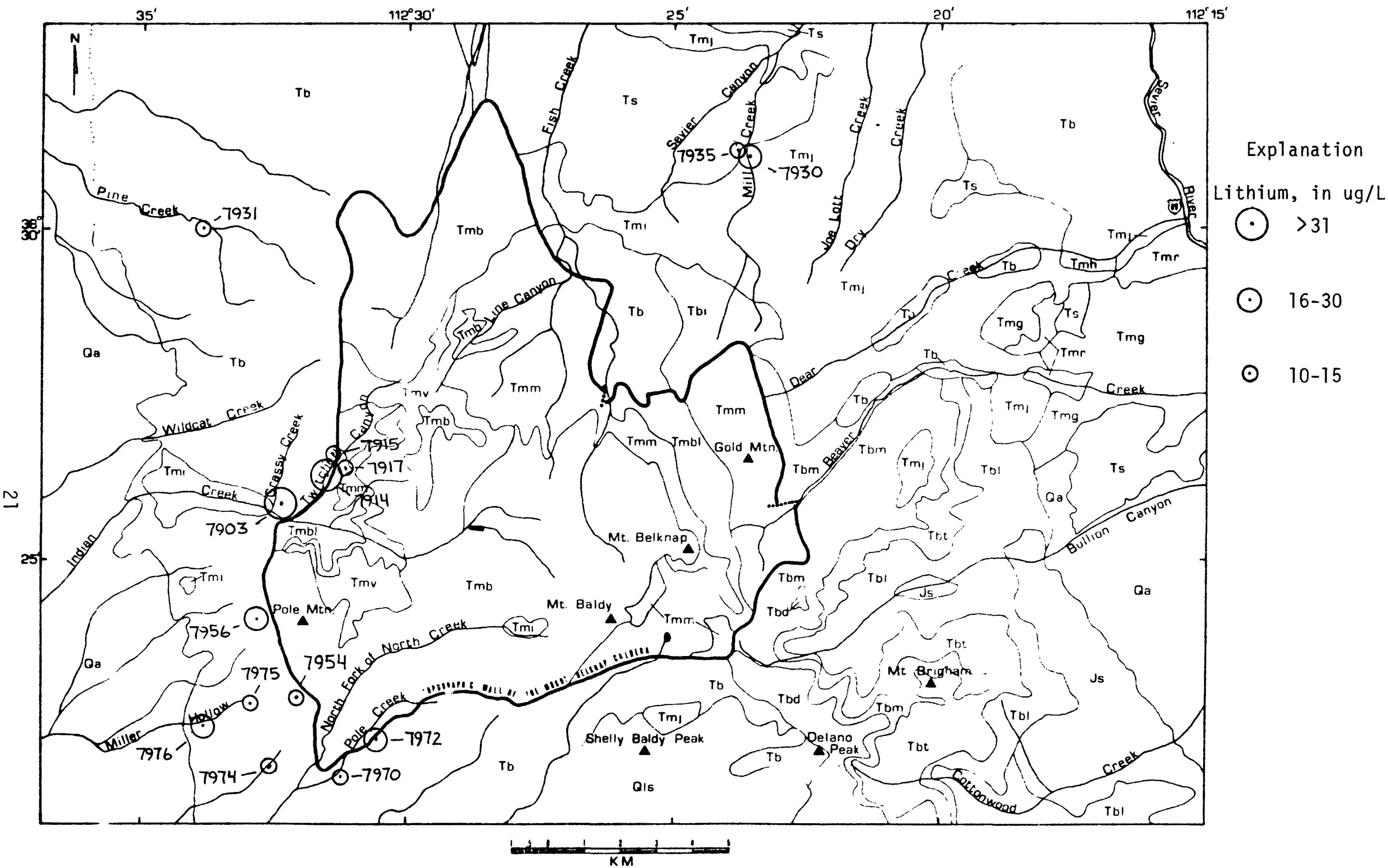

Figure 10 -- Distribution of anomalous lithium concentrations in the Mount Belknap caldera area , Utah. Numbers are those of sample sites. See figure 2 for description of geologic units.

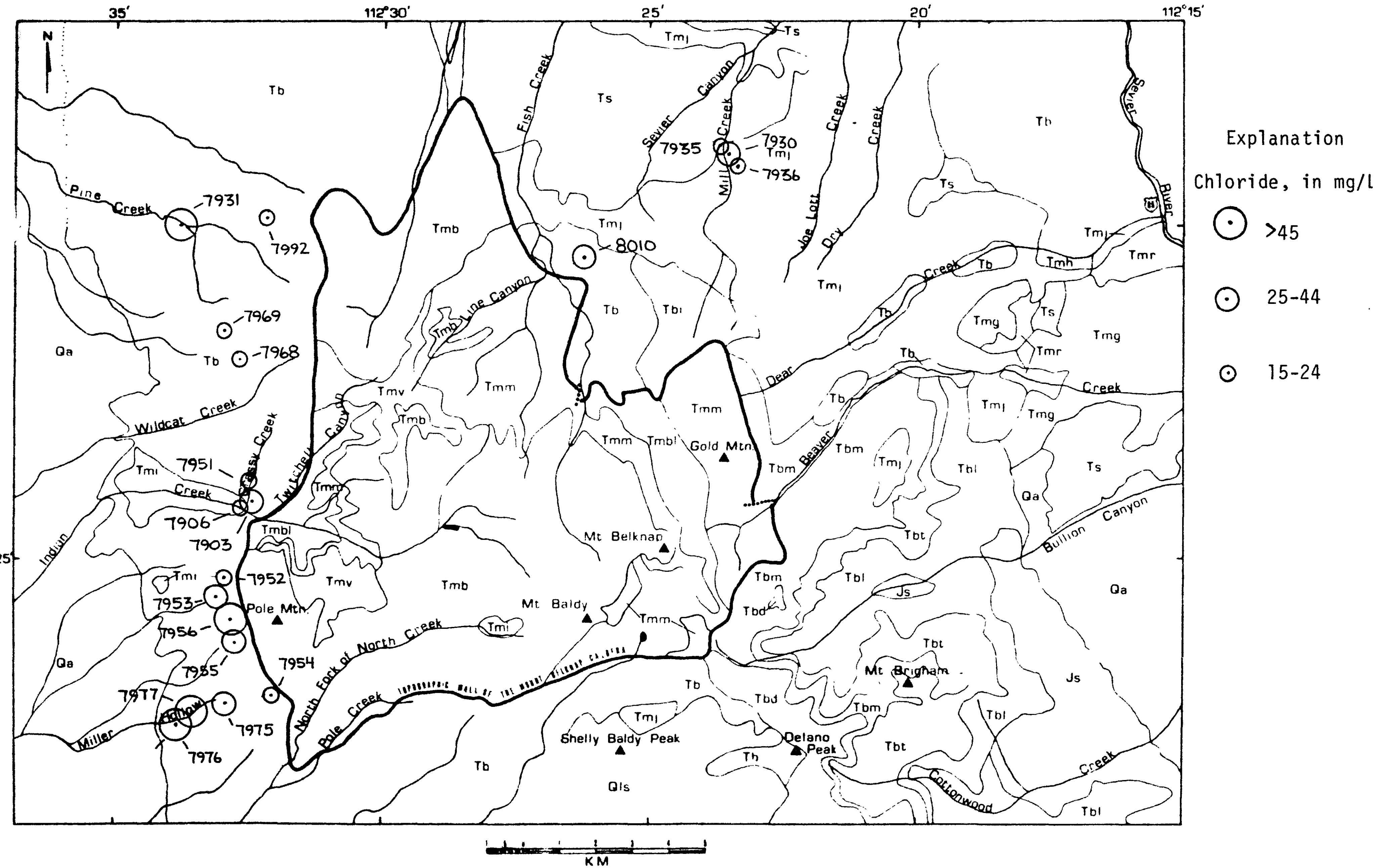

Figure 11 -- Distribution of anomalous chloride concentrations in the Mount Belknap caldera area, Utah. Numbers are those of sample sites. See figure 2 for description of geologic units.

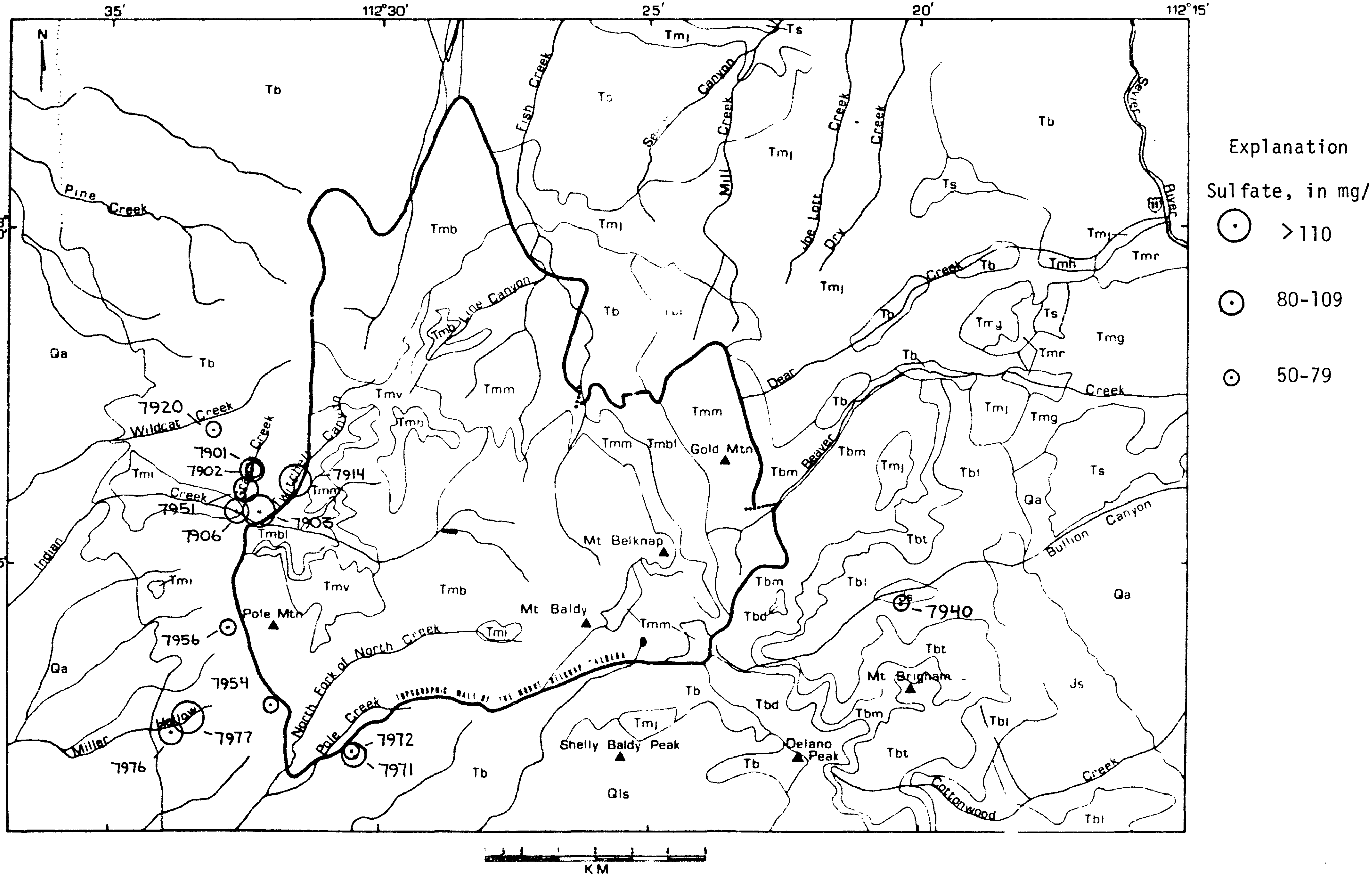

Figure 12 -- Distribution of anomalous sulfate concentrations in the Mount Belknap caldera area, Utah. Numbers are those of sample sites. See figure 2 for description of geologic units.

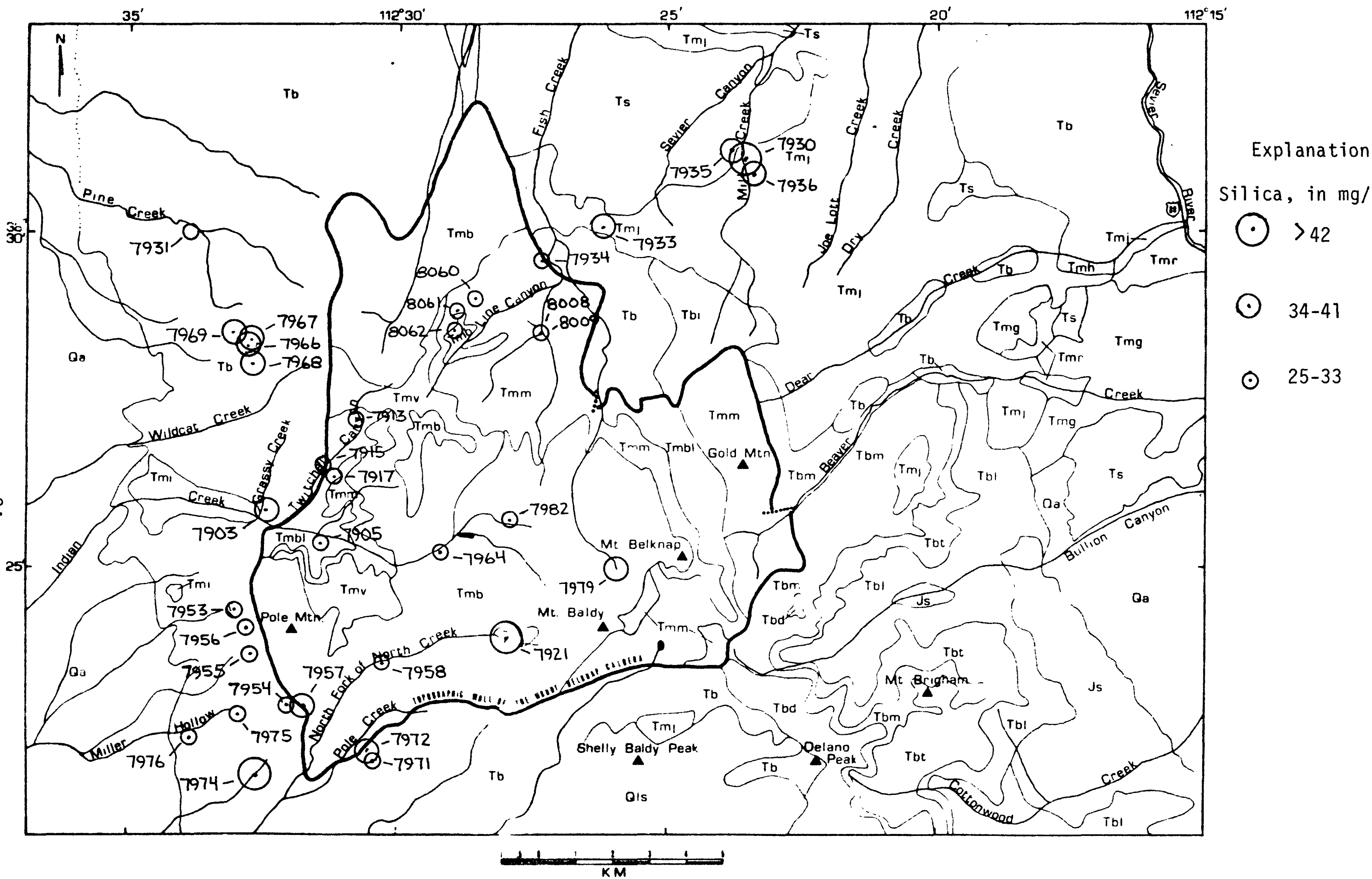

Figure 13 -- Distribution of anomalous silica concentrations in the Mount Belknap caldera area, Utah. Numbers are those of sample sites. See figure 2 for description of geologic units.

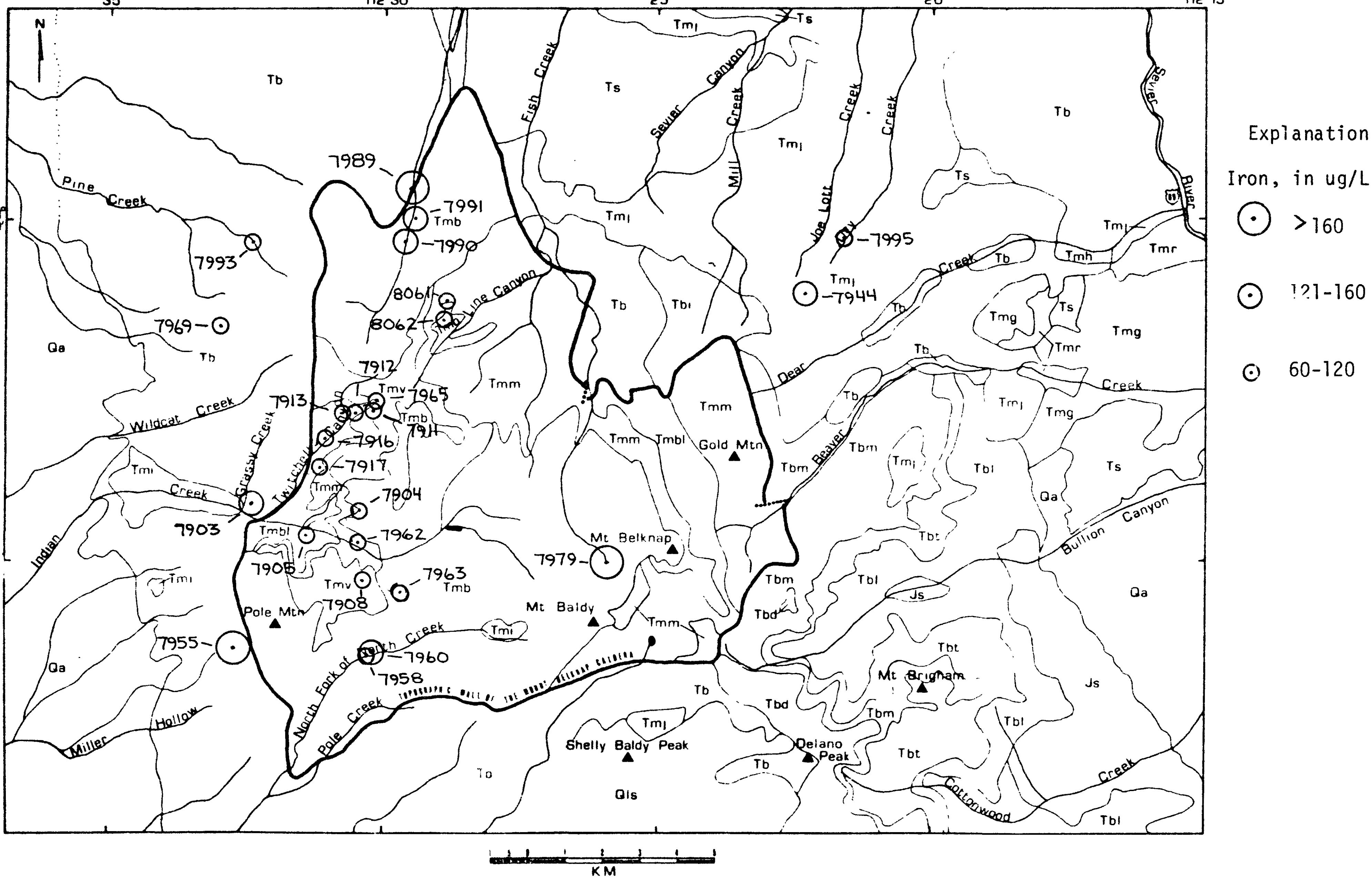

Figure 14 -- Distribution of anomalous iron concentrations in the Mount Belknap caldera area, Utan. Numbers are those of sample sites. See figure 2 for description of geologic units.

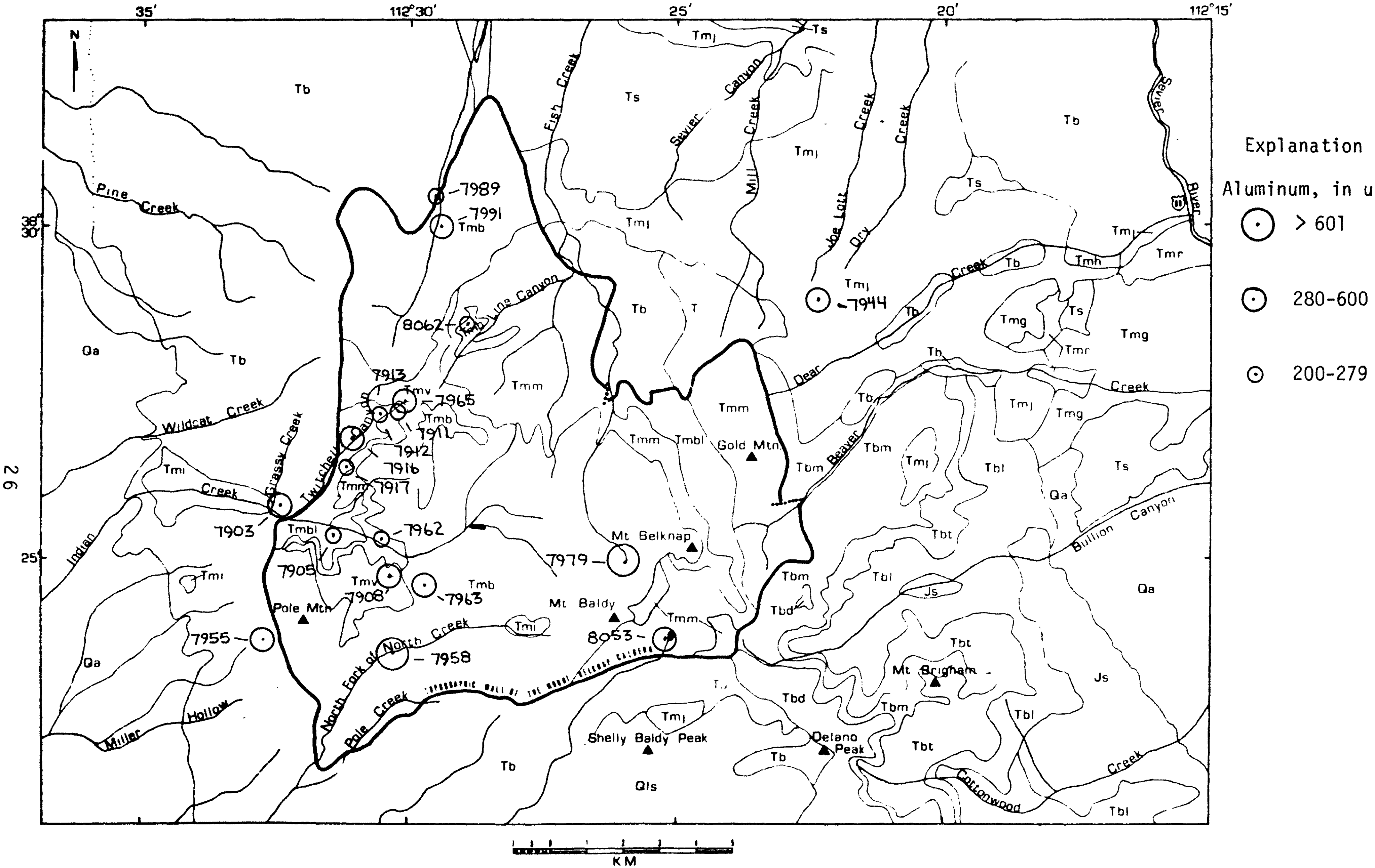

Figure 15 -- Distribution of anomalous aluminum concentrations in the Mount Belknap caldera area, Utah. Numbers are those of sample sites. See figure 2 for description of geologic units.

Copper concentrations are high in three distinct places: (1) Bullion Canyon, (2) Kimberly area, and (3) along the western margin, particularly near Twitchell Canyon (fig. 16). The highest values occur at sample sites 7908, 7903, 7914, 7901, 7941, 7940, and 7902 with concentrations of 9.2, 5.7, 4.5, 4.4, 4.2, 4.1, and 4.0 μg/L, respectively. Moderately anomalous copper concentrations are found in the Bullion Canyon area, Miller Hollow, Pole Creek, Grassy Creek, and Kimberly areas.

The most anomalous lead concentrations are from sample sites 7921 and 7907, with values of 5.8 and 4.1 μg/L, respectively. Moderately anomalous lead values are restricted to the caldera with the exception of sample site 7944 (fig. 17).

The most anomalous zinc concentrations occur in samples 7903 and 7979, with values of 290 μg/L and 180 μg/L, respectively. Moderately anomalous values occur in the Twitchell Canyon and Pole Canyon areas, in the caldera, and in sample 7966 (fig. 18).

The most anomalous manganese concentrations occur at sample sites 7979, 7903, and 7960, with values of 2.3, 1.8, and 0.74 μg/L, respectively. Moderately anomalous values occur in Miller Hollow, in the caldera, and at single points along the western margin (fig. 19).

The most anomalous barium concentrations occur along the western margin of the caldera, the highest values occur along the western margin and Mill Creek (fig. 8).

Anomalous fluoride concentrations are restricted primarily to the caldera or its periphery, except sample 7930 (fig. 20). The most anomalous value is 27 mg/L from sample 7903. Moderately anomalous concentrations occur at sample sites 7906, 7914, 7979, 8058, 7960, and 7958, with values of 4.2, 2.9, 2.5, 1.9, 1.9, and 1.5 mg/L, respectively.

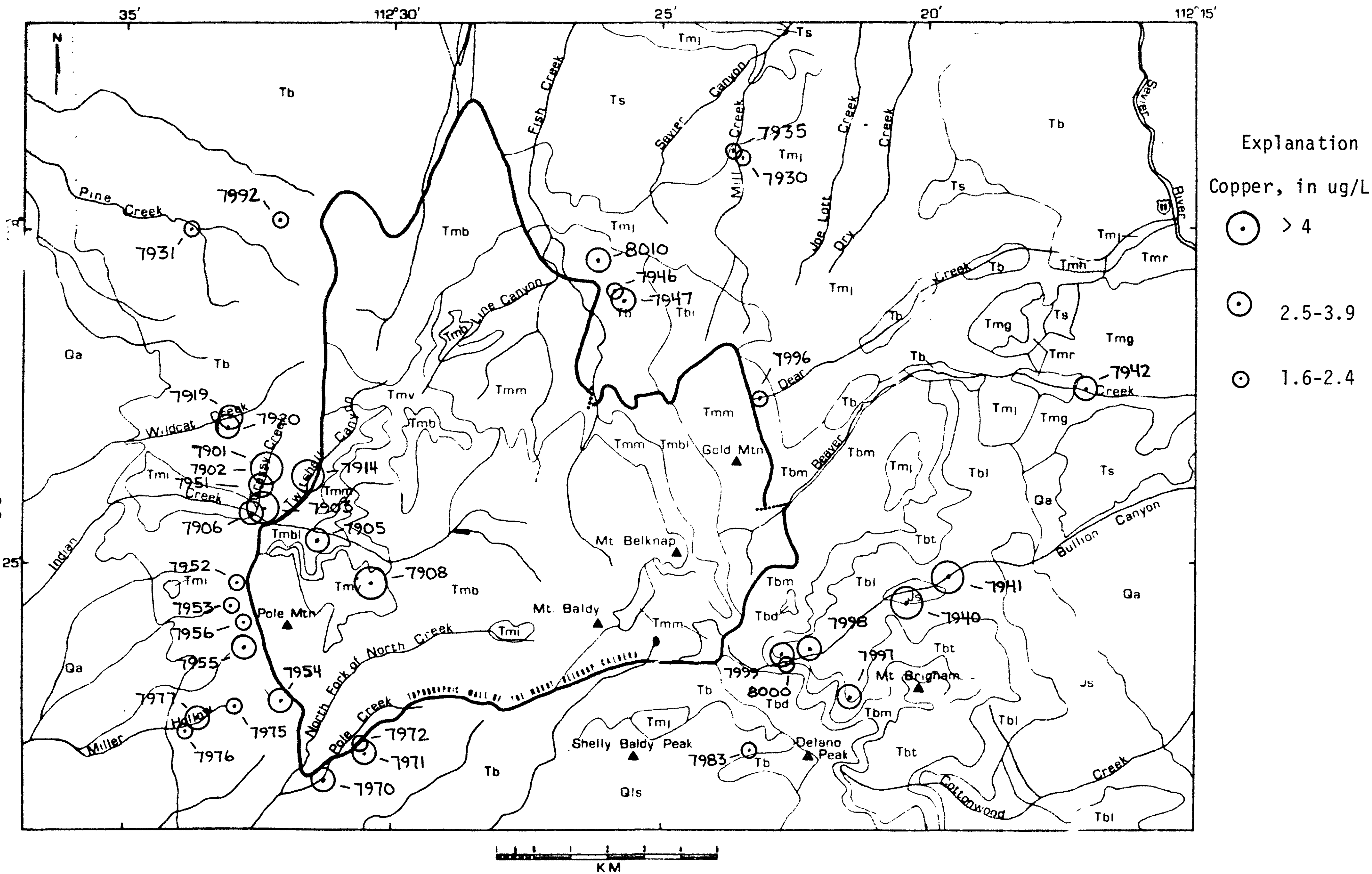

Figure 16 -- Distribution of anomalous copper concentrations in the Mount Belknap caldera area, Utah. Numbers are those of sample sites. See figure 2 for descriptions of geologic units.

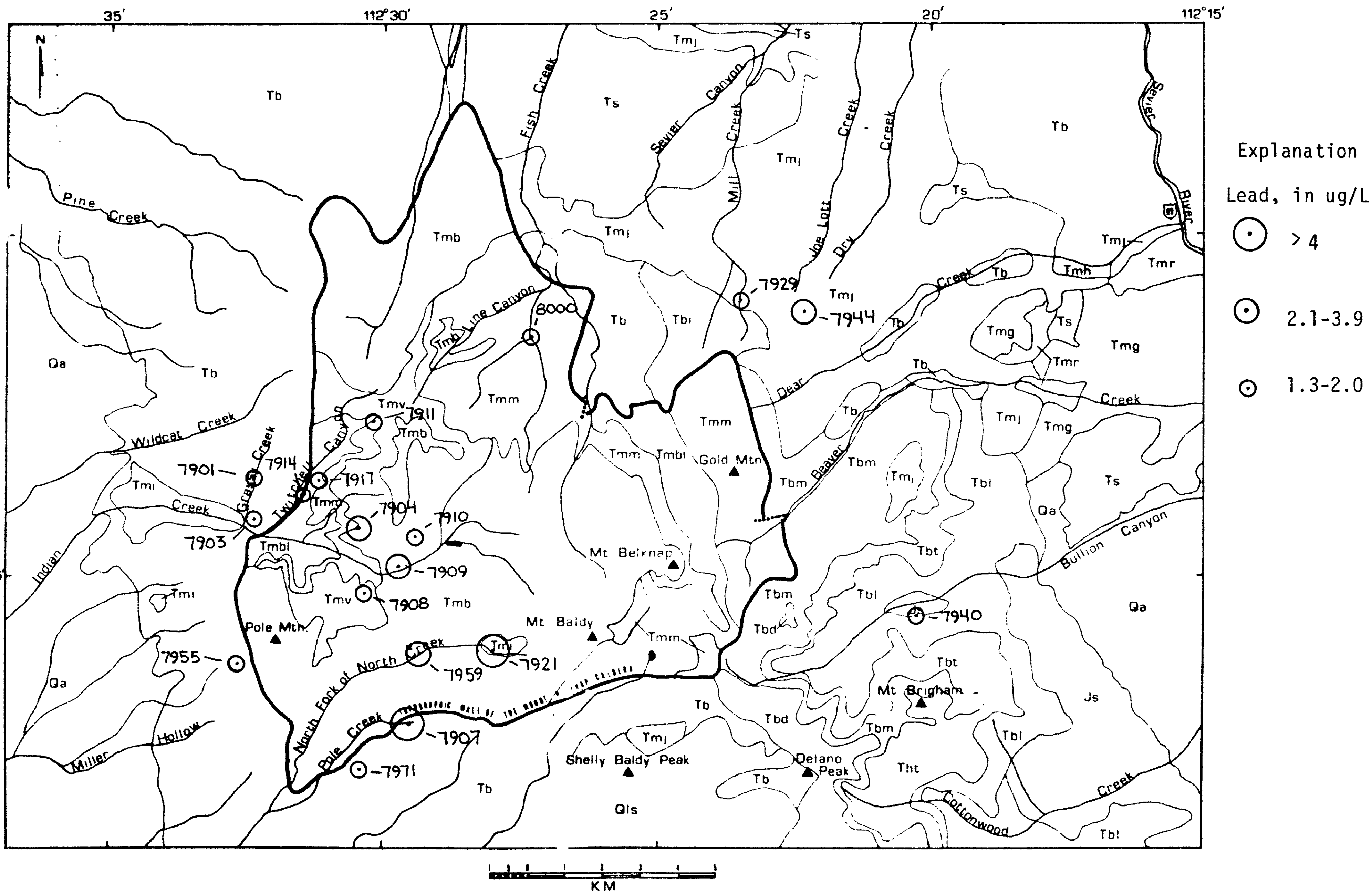

Figure 17 -- Distribution of anomalous lead concentrations in the Mount Balknap caldera area, Utah. Numbers are those of sample sites. See figure 2 for description of geologic units.

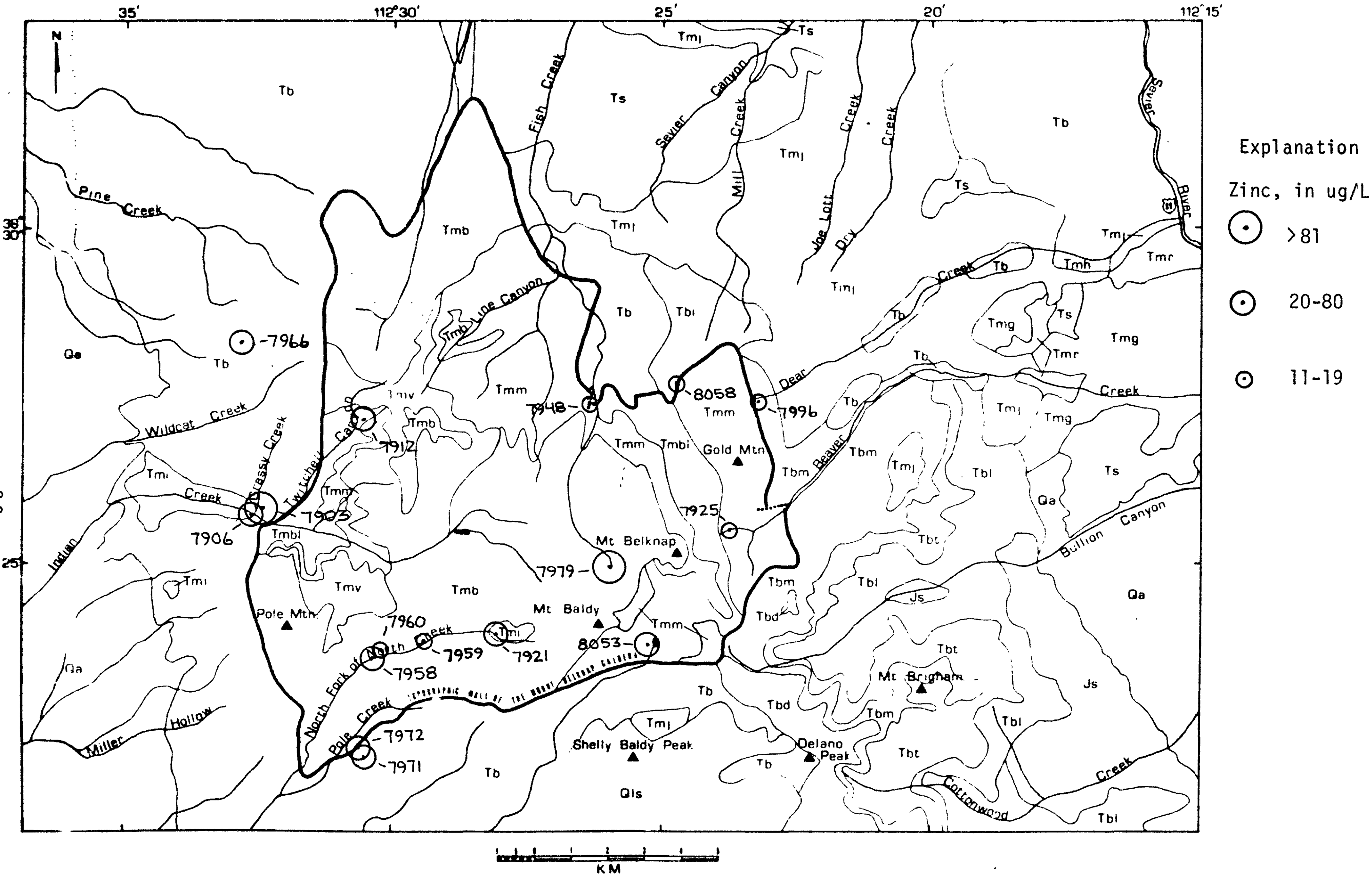

Figure 18 -- Distribution of anomalous zinc concentrations in the Mount Belknap caldera area, Utah. Numbers are those of sample sites. See figure 2 for description of geologic units.

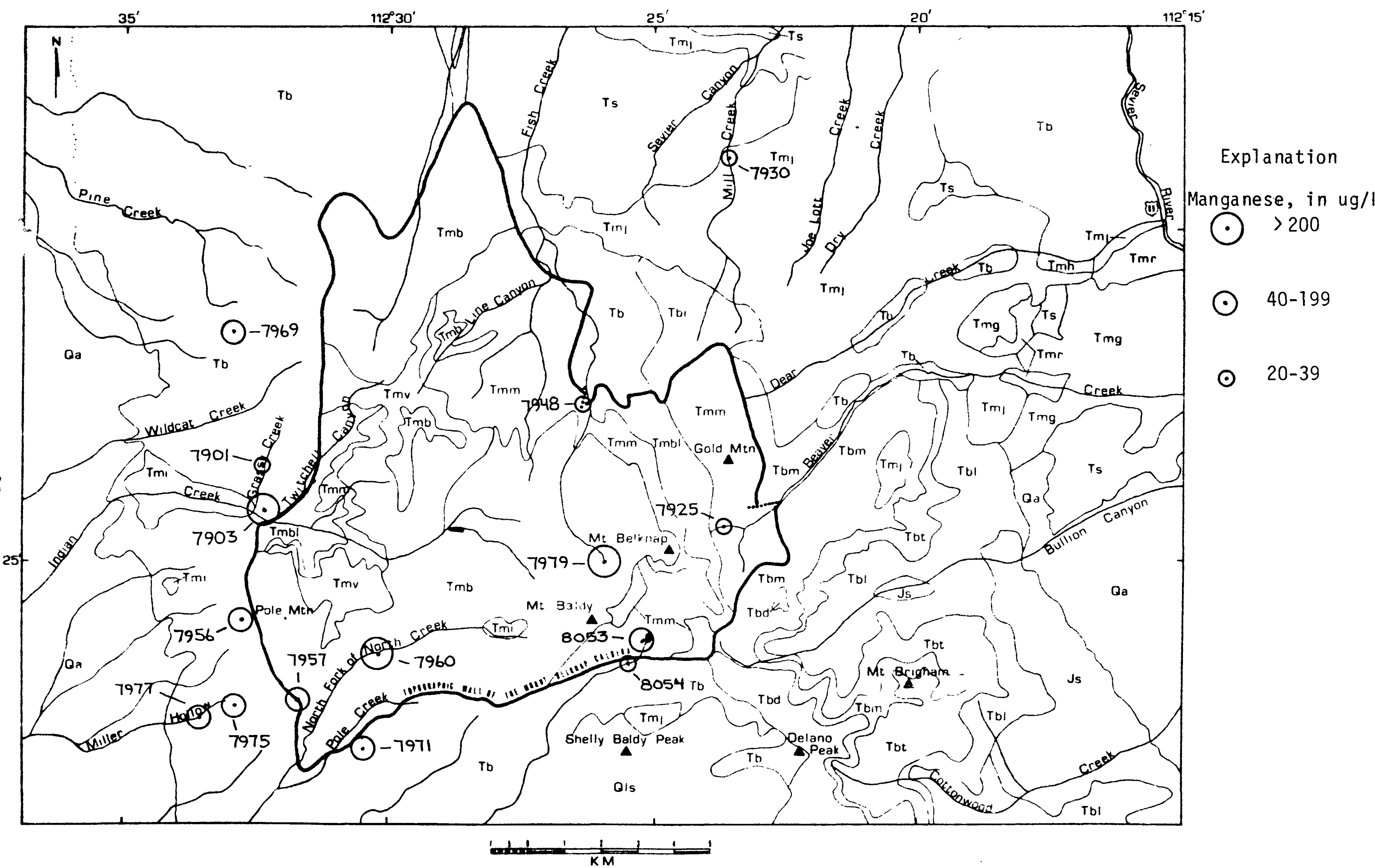

Figure 19 -- Distribution of anomalous manganese concentrations in the Mount Belknap caldera area, Utah. Numbers are those of sample sites. See figure 2 for description of geologic units.

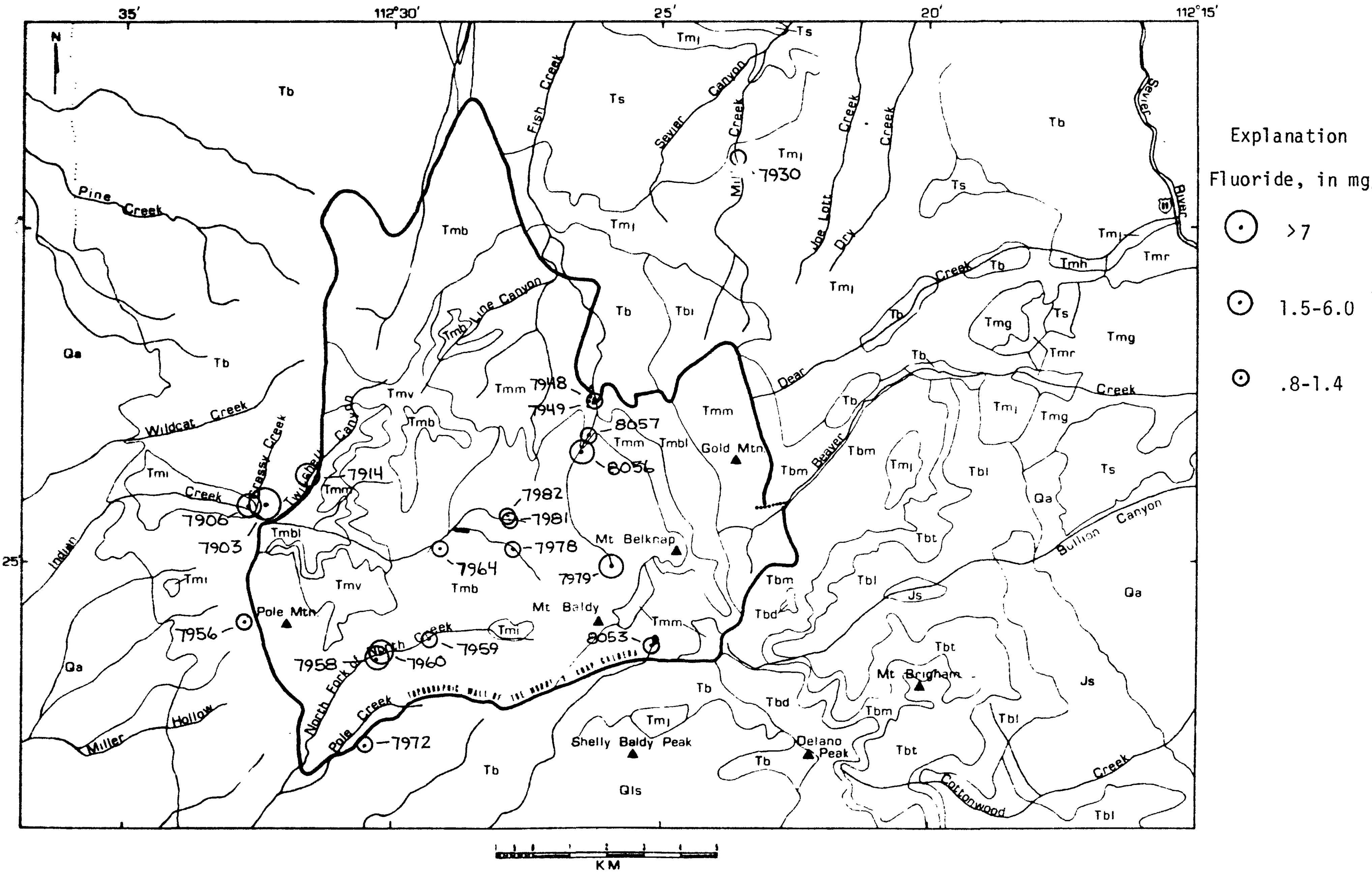

Figure 20 -- Distribution of anomalous fluoride concentrations in the Mount Belknap caldera area, Utah. Numbers are those of sample sites. See figure 2 for description of geologic units.

Anomalous beryllium values occur at sample sites 7903, 7979, and 7958 with concentrations of 26, 9.5, and 6 g/L, respectively. The moderately anomalous values are restricted to the caldera (fig. 21).

The most anomalous uranium concentration is from sample 7903, with 490 g/L. Samples 7906 and 7920 have concentrations of 200 ppb and 20 g/L, respectively. Moderately anomalous uranium values occur in Miller Hollow, and at sample site 7992 (fig. 22).

The most anomalous molybdenum concentrations occur in samples 7914 and 7943, with 6.8 g/L and 2.4 g/L, respectively. There are no distinct trends in molybdenum concentrations (fig. 23). The temperature ranges from 2° to 23°C. The pH ranges from 4.4 to 8.55.

The single-element plots indicate that certain areas contain anomalous concentrations of many constituents. The Grassy Creek-Twitchell Canyon area has anomalous concentrations of lithium, sodium, calcium, sulfate, potassium, aluminum, copper, zinc, manganese, fluoride, beryllium, uranium, and molybdenum. This area is designated the Grassy Creek anomaly. Another area, designated the Miller Hollow anomaly, has anomalous concentrations of boron, sodium, magnesium, calcium, chloride, sulfate, barium, and moderately anomalous uranium. Some of the samples in Pole Creek, including 7974, and the few samples in the north fork of North Creek, have anomalous concentrations of boron, potassium, silica, aluminum, manganese, beryllium, and uranium. This large area is designated the Pole Creek anomaly. However, the samples in the north fork of North Creek are from within the caldera and may have a different geochemical history than the samples in Pole Creek, which are not in the caldera. One or more of the samples in Mill Creek have anomalous concentrations of sodium, silica, and molybdenum. This area is designated the Mill Creek anomaly.

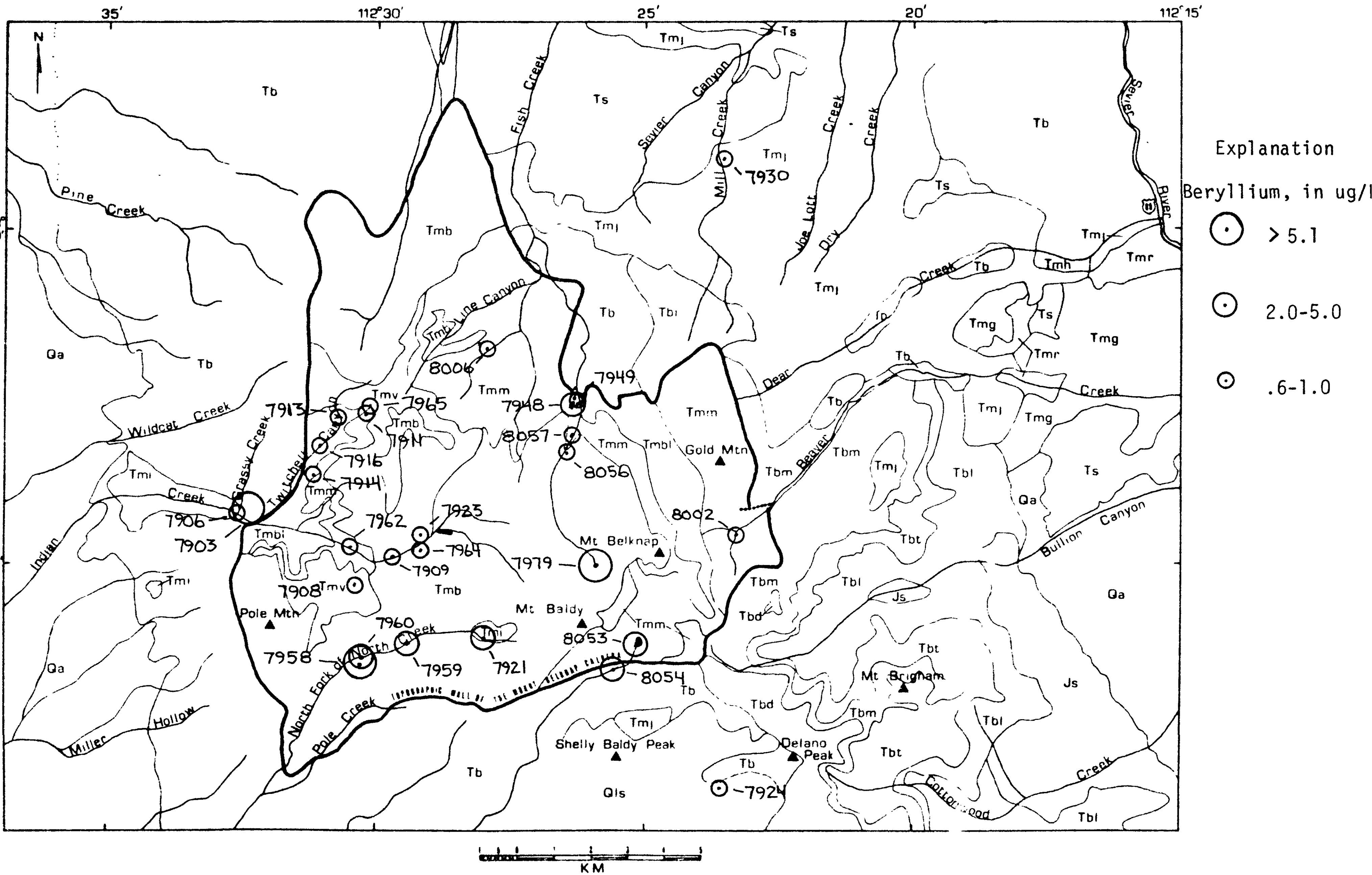

Figure 21 -- Distribution of anomalous beryllium concentrations in the Mount Belknap caldera area, Utah. Numbers are those of sample sites. See figure 2 for description of geologic units.

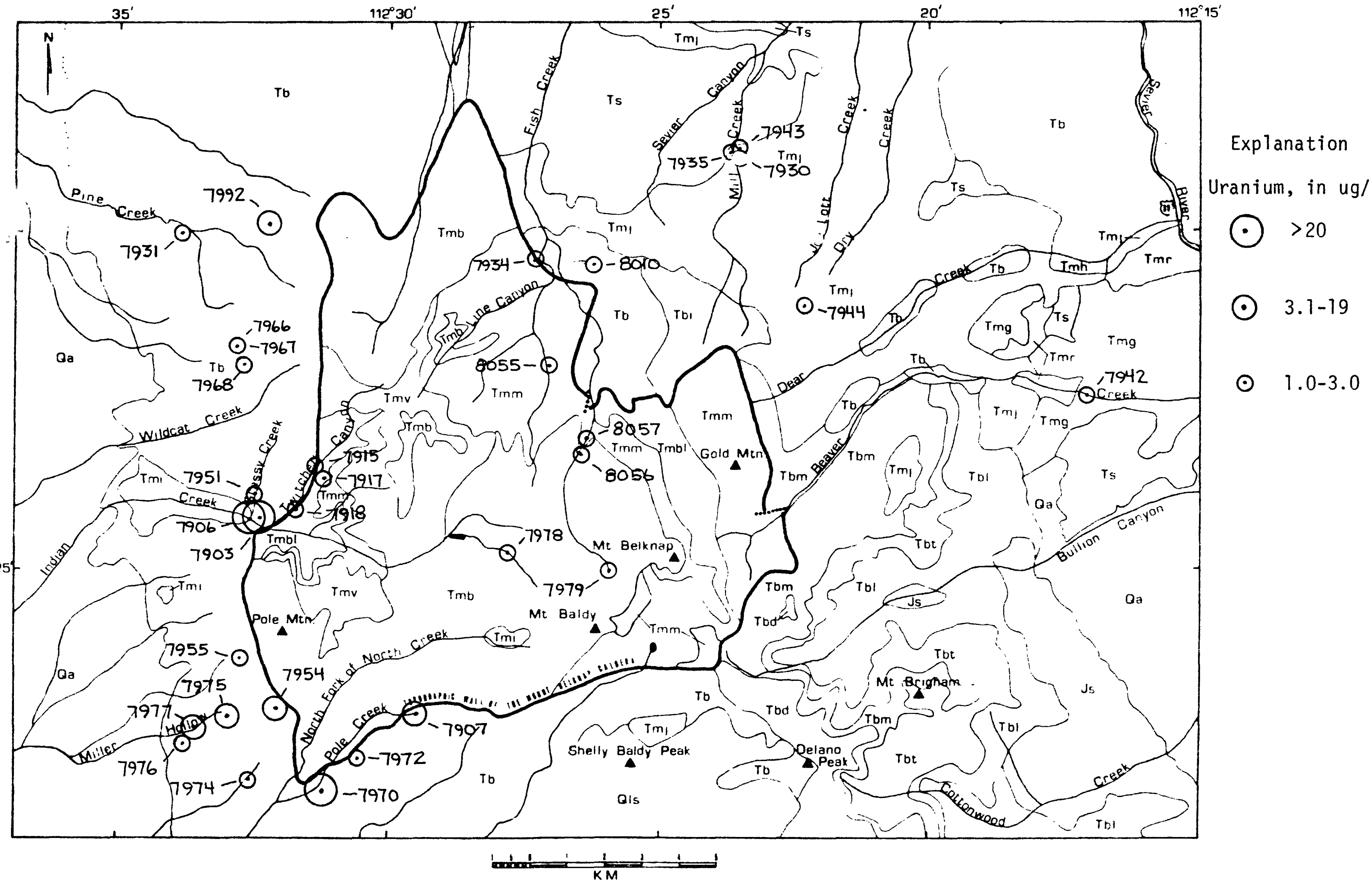

Figure 22 -- Distribution of anomalous uranium concentrations in the Mount Belknap caldera area, Utah. Numbers are those of sample sites. See figure 2 for description of geologic units.

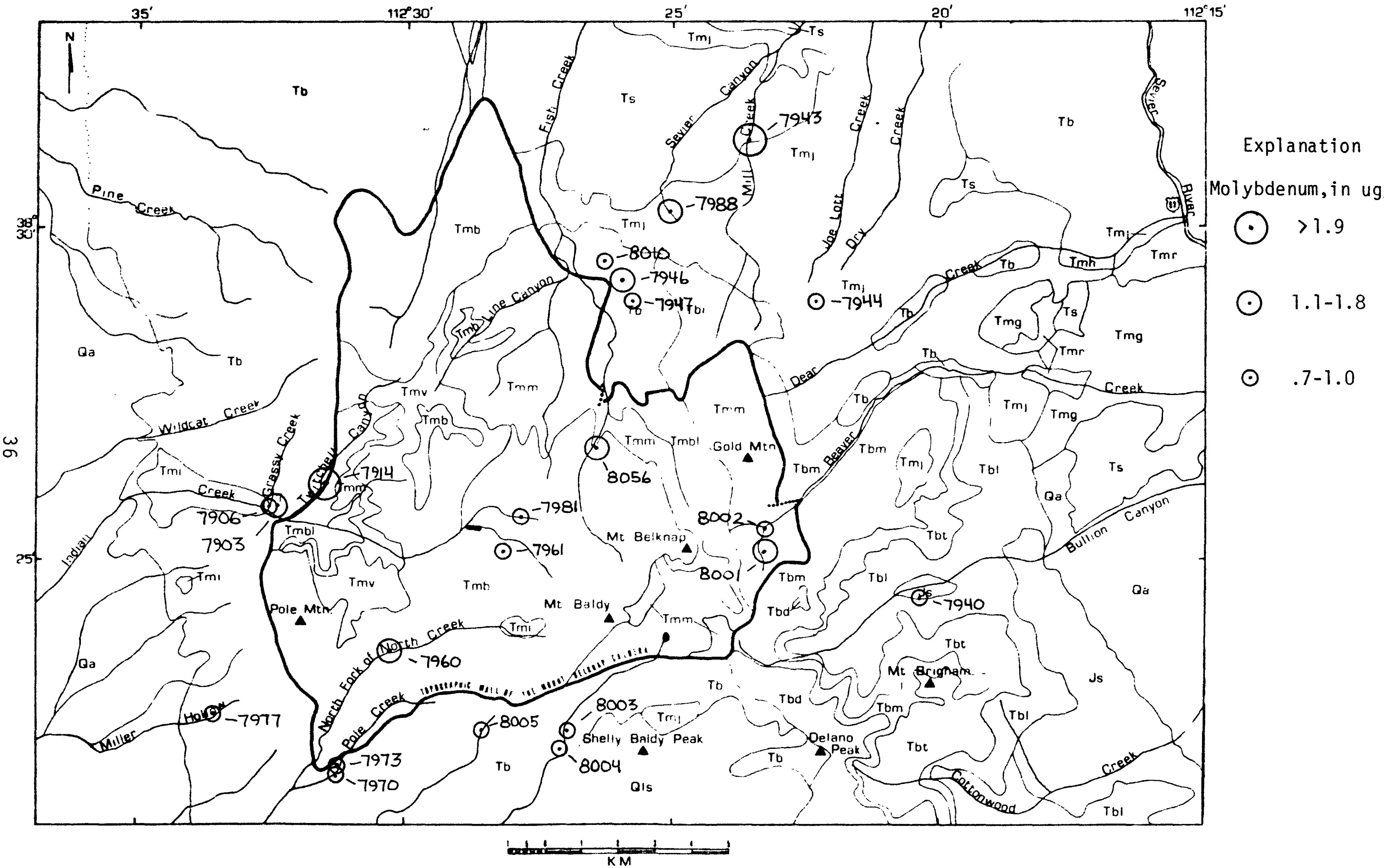

Figure 23 -- Distribution of anomalous molybdenum in the Mount Belknap caldera area, Utah. Numbers are those of sample sites. See figure 2 for description of geologic units.

Of the four anomalous areas identified using the single plots, the most significant is the Grassy Creek anomaly, followed in importance by the Miller Hollow, Pole Creek, and Mill Creek anomalies.

CHEMICAL MODELING OF THE WATERS

The water in the area is undoubtedly of meteoric origin. The different water chemistries are related to the chemical weathering of the host rock. Chemical modeling and determinations of the species of metal complexes of many of the samples was done using the WATEQ2 program (Ball, 1980). WATEQ2 uses thermodynamic data and constituent concentrations to calculate the most probable speciation that would exist under equilibrium conditions. The WATEQ2 results for waters from springs indicate that carbonate, fluoride, and sometimes hydroxide are the principle metal-complexing anions. Examples of springs in which fluoride complexes predominate are: 7903, 7978, 7979, and 7958. Examples of springs in which carbonate complexes predominate are: 7912, 7930, 7956, and 7962. Carbonate or bicarbonate are the predominate-complexing anion in the stream waters. The stream-water chemistry is more complex because both surface and ground water contribute to the total stream flow.

The correlation matrix for the log-transformed data from spring waters is shown in table 6. Correlation coefficients with alkalinity, which is primarily a measure of the bicarbonate ion, compared with Ca, Mg, Ba, Sr, and Cl, is greater than 0.40. Correlation coefficients with fluoride compared with K, Li, Be, SiO_2, SO_4, Zn, Mn, Al, and U, is greater than 0.45. Those springs containing anomalous concentrations of the alkali-earth metals and boron are located in the area just west of the caldera, in the Kimberly area, and along the caldera periphery; examples are 7955, 7956, 7974, and 8010. The

Table 6--Correlation coefficients and number of pairs

	Ca	Mg	Na	K	Li	Sr	Ba	B	Be	SiO_2	Alk	SO_4	Cl	F	Zn	Cu	Mo	Pb	As	Fe	Mn	Al	U
Ca(mg/L)	0.52	0.94	0.81	0.35	0.55	0.91	0.80	0.31	0.27	0.35	0.51	0.68	0.82	0.14	0.04	0.86	0.29	-0.20	0.82	-0.57	-0.04	0.06	0.62
Mg(mg/L)	39	0.60	0.78	0.38	0.54	0.90	0.76	0.36	0.31	0.35	0.45	0.69	0.79	0.12	0.05	0.78	0.34	-0.10	0.71	-0.48	0.04	0.09	0.55
Na(mg/L)	39	39	0.39	0.50	0.63	0.74	0.62	0.57	0.20	0.67	0.35	0.68	0.89	0.36	0.16	0.68	0.33	-0.06	0.73	-0.38	0.04	0.15	0.56
K (mg/L)	39	39	39	0.42	0.30	0.15	0.23	0.22	0.82	0.75	-0.19	0.68	0.60	0.49	0.53	0.39	0.17	0.27	0.44	0.14	0.32	0.25	0.26
Li(ug/L)	30	30	30	30	0.39	0.46	0.43	0.26	0.52	0.38	-0.15	0.72	0.58	0.59	0.34	0.64	0.41	0.08	0.64	-0.19	0.70	0.19	0.63
Sr(ug/L)	39	39	39	39	30	0.67	0.87	0.36	0.08	0.23	0.61	0.55	0.72	0.01	-0.15	0.70	0.28	-0.34	0.62	-0.55	-0.10	-0.02	0.53
Ba(ug/L)	31	31	31	31	24	31	0.64	0.54	0.29	0.14	0.44	0.59	0.59	0.01	-0.06	0.68	0.32	-0.20	0.58	-0.42	-0.02	-0.07	0.40
B (ug/L)	14	14	14	14	14	14	13	0.21	-1.00	0.56	0.37	0.07	0.41	-0.20	-0.23	-0.09	-0.10	-0.26	-0.07	-0.19	-0.08	-0.56	-0.19
Be(ug/L)	12	12	12	12	8	12	10	2	0.51	0.47	-0.89	0.81	0.06	0.90	0.93	0.37	0.56	0.18	0.61	0.55	0.69	0.84	0.69
SiO2(mg/L)	39	39	39	39	30	39	31	14	12	0.25	0.01	0.47	0.66	0.46	0.39	0.21	0.06	0.18	0.45	0.05	0.27	0.36	0.35
Alk(mg/L)	39	39	39	39	30	39	31	14	12	39	1.54	-0.14	0.40	-0.54	-0.63	0.24	-0.18	-0.29	0.13	-0.53	-0.55	-0.33	0.05
SO4(mg/L)	39	39	39	39	30	39	31	14	12	39	39	0.64	0.68	0.59	0.53	0.71	0.44	0.01	0.69	-0.16	0.48	0.26	0.58
Cl(mg/L)	39	39	39	39	30	39	31	14	12	39	39	39	0.68	0.29	0.07	0.65	0.27	-0.08	0.70	-0.35	-0.07	0.08	0.53
F (mg/L)	39	39	39	39	30	39	31	14	12	39	39	39	39	0.51	0.74	0.22	0.39	0.22	0.42	0.21	0.60	0.55	0.57
Zn(ug/L)	39	39	39	39	30	39	31	14	12	39	39	39	39	39	0.51	0.15	0.26	0.29	0.31	0.36	0.59	0.64	0.37
Cu(ug/L)	39	39	39	39	30	39	31	14	12	39	39	39	39	39	39	0.47	0.27	-0.05	0.85	-0.45	0.12	-0.00	0.59
Mo(ug/L)	39	39	39	39	30	39	31	14	12	39	39	39	39	39	39	39	0.16	-0.10	0.33	0.00	0.54	0.36	0.52
Pb(ug/L)	28	28	28	28	22	28	23	9	11	28	28	28	28	28	28	28	28	0.17	-0.02	0.43	0.14	0.31	-0.04
As(ug/L)	39	39	39	39	30	39	31	14	12	39	39	39	39	39	39	39	39	28	0.22	-0.48	0.11	0.29	0.71
Fe(ug/L)	39	39	39	39	30	39	31	14	12	39	39	39	39	39	39	39	39	28	39	0.66	0.47	0.65	-0.17
Mn(ug/L)	19	19	19	19	17	19	17	11	7	19	19	19	19	19	19	19	19	13	19	19	0.90	0.46	0.46
Al(ug/L)	24	24	24	24	17	24	18	6	11	24	24	24	24	24	24	24	24	20	24	24	12	0.53	0.60
U (ug/L)	34	34	34	34	28	34	27	14	10	34	34	34	34	34	34	34	34	24	34	34	17	20	0.70

note: the diagonal of the correlation matrix contains the standard deviation of the variable for only the valid pairs chemical character of these springs is indicative of the chemical weathering of intermediate-composition rocks that may have been hydrothermally altered. The spring waters containing anomalous concentrations of fluoride, lithium, zinc, molybdenum, and uranium are generally located within the caldera or near its periphyry. The chemical character of these springs is indicative of the chemical weathering of silicic rocks which possibly contain sulfide and (or) uranium minerals. Springs of this type are: 7903, 7930, 7958, 7979, and 8053. Those springs that have few anomalous constituent values probably reflect the influence of normal chemical weathering in barren rock. Springs of this type are: 7909, 7984, and 7985.

There is evidence that some of the area has been hydrothermally altered (Cunningham and Steven, 1979d). The warm temperatures and high silica content of some of the springs indicate that a high heat flow may still exist under parts of the area. Springs that fit this criteria are: 7974, 7976, 7930, 7903, 7935, and 7955. The chemistry of some small streams may be affected by warm springs or the weathering of mineralized areas, examples are: 7933, 7921, 7936, and 7979.

The water chemistry indicates that there are significant differences in host-rock chemistry and that three major types of springs exist in the area. Most of the water chemistry of the springs reflects the influence of normal chemical weathering. A second group of springs has anomalous concentrations of alkali and alkali-earth elements and boron; these springs are commonly associated with hydrothermally altered areas. The third group of springs has anomalous concentrations of many of the lithophile elements and constitutents associated with the weathering of silicic rocks containing sulfides, or possibly uranium minerals.

MULTIVARIANT ANALYSIS APPLIED TO THE WATER DATA

Each water sample constitutes a multispecie set of data. Q-mode factor analysis techniques are used to gain a better understanding of the complex interrelationships within the data. Q-mode factor analysis is a mathematical technique that calculates a group of end-member compositions or principal components that approximately describe the variations within the multispecies data. Each end-member then will represent a unique set of parameters or chemical controls that affect the water chemistry. For a detailed discussion of Q-mode factor analysis, as applied to water geochemistry, see Miller and others (1979).

The Q-mode analysis technique demonstrates that certain factors exist but does not attach any significance to them. The interpretation of the factors and their geological significance is a subjective process which relies on the users knowledge of the geology and geochemistry of the area. Background information and the application of factor analysis to geochemical studies can be found in Davis (1973); Miller and Ficklin (1976); and Miller and others (1980).

Q-mode factor analysis was carried out, using the U.S. Geological Survey's STATPAC library system. The basic algorithms for the program are from Klovan and Imbrie (1971). The raw data was summed to 100 prior to factor analysis. A four-factor model, which explains 92.2 percent of the variation, was used in interpreting the data. Table 7 is the factor loading matrix.

Table 6.--Factor loading matrix
[Significant loadings are underlined]

Factor	1	2	3	4
Ca	0.4454	-0.0666	-0.2706	0.1516
Mg	0.1588	-0.0235	-0.2301	-0.1111
Na	-0.0180	0.3978	-0.0415	-0.5062
K	-0.0490	0.2650	-0.1148	-0.0479
Li	-0.0093	0.0792	-0.1253	-0.1282
SiO_2	-0.1005	0.4851	0.2399	-0.0927
Alkalinity	0.6046	-0.0696	0.5396	-0.2504
SO_4	0.0071	0.1085	-0.4367	0.1286
Cl	0.0303	0.0319	-0.1759	-0.3569
F	-0.0811	0.2670	-0.1063	0.1896
Zn	-0.0357	0.1104	-0.0471	0.0756
Cu	0.0625	0.0423	0.0164	0.1155
Mo	0.0159	0.3580	0.2876	0.4209
As	0.0213	0.2373	0.1687	0.2094
Fe	-0.0373	0.1217	0.0664	-0.0529
Mn	-0.0193	0.0347	-0.0562	0.0250
Al	-0.0519	0.1637	-0.0565	0.0178
U	0.0026	0.0155	-0.1549	0.0358
Conductivity	0.5208	0.3490	-0.2963	-0.0812
Ba	0.2424	-0.0389	-0.0616	0.3325
Be	-0.0600	0.1397	-0.1154	0.0705
B	0.0449	0.2262	0.0860	0.1385
Sr	0.2109	-0.0233	-0.0297	0.2284

Factors 1 and 2

Factors 1 and 2, which have been interpreted as representing lithologic controls, account for almost 86 percent of the variation of the multispecie data. Factor 1 explains 49.4 percent of the total variance. It is interpreted as representing the chemical weathering of intermediate-composition rocks. The distribution of factor-1 scores is shown in figure 24 and is mainly restricted to rock in the outer walls of the caldera. Factor 2 explains 36.4 perecent of the total variance. This factor is interpreted as representing the chemical weathering of silicic rocks. The distribution of factor-2 scores is shown in figure 25 and is restricted to the core of the caldera.

Factor 3

Factors 3 and 4 contain loadings of elements commonly associated with mineralization. Factor 3 explains 2.49 percent of the total variance. The highest loading for U, Mg, Cl, SO_4, Li, Mn occur in this factor. Ca, K, Be, F, Ba, Al, Zn, and Sr, also have high loadings in this factor. This factor is interpreted as reflecting uranium mineralization. The highest factor scores occur at sample sites 7971, 7903, 7951, 7956, 7972, 7906, 7914, 7901, and 7902 with scores of 0.49, 0.48, 0.42, 0.37, 0.36, 0.36, 0.35, 0.34, and 0.33, respectively. Figure 26 gives the distribution of the highest scores for factor-3 scores.

The Grassy Creek anomaly contains a clustering of high scores for factor 3. Another clustering of high-factor scores occurs at the Pole Creek anomaly. Two clusterings of slightly less anomalous factor scores occur in the Big Meadow area--designated the Big Meadow anomaly--and in the Miller Hollow anomaly. High values of scores for factor 3 occur at several localities within the caldera and near the periphery.

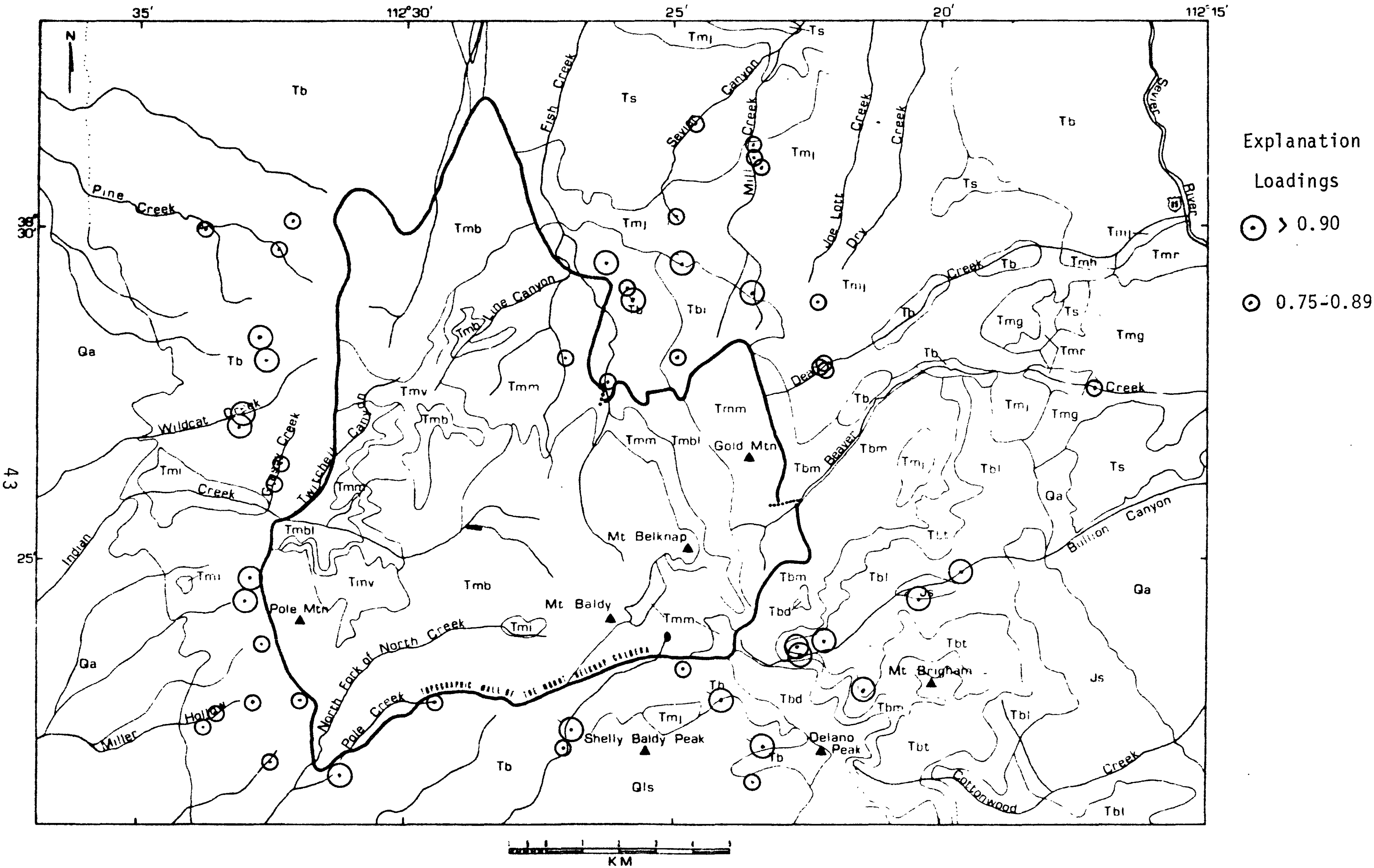

Figure 24 -- Disrtibution of scores for factor 1. See figure 2 for description of geologic units.

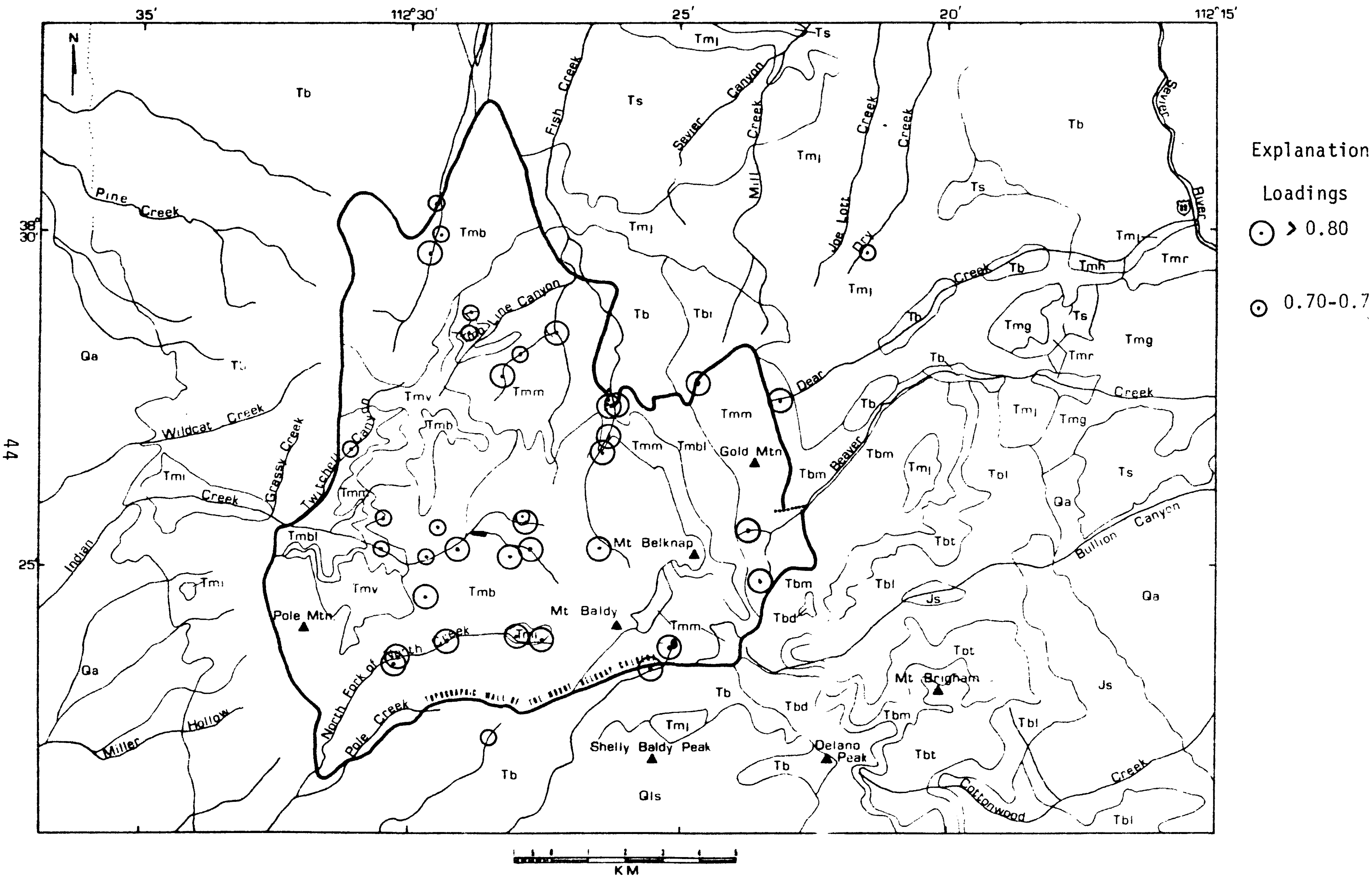

Figure 25 -- Distribution of scores for factor 2. See figure 2 for description of geologic units.

Two possible origins are postulated for the uranium mineralization. The uranium mineralization may be related to hydrothermal activity that mobilized uranium contained in caldera-filling rocks shortly after the caldera collapse. Samples 7964, 7921, 7958, 7960, and 7948 may be examples of waters in contact with this type of mineralization. Some of the high scores for factor 3 of samples from around the caldera periphyry may be related to this type of mineralization, such as the Pole Creek, Miller Hollow, or Grassy Creek anomalies. An origin more directly related to an intrusive body at depth, as postulated by Cunningham and Steven (1979b) for the Alunite Ridge area, is a second possible origin of the uranium.

Factor 4

Factor 4 explains 3.89 percent of the total variance. The highest loadings for Mo, Cu, Ba, and Sr occur in factor 4 (table 7). This factor is interpreted as reflecting molybdenum mineralization, possibly related to a porphyry molybdenum-type system. The highest scores are from 7986, 7945, 8001, 7999, 8002, 7941, 7997, and 7925 with factor scores of 0.23, 0.23, 0.23, 0.17, 0.16, 0.16, 0.14, 0.13, 0.11, and 0.11, respectively. Figure 27 shows the distribution of the anomalous factor scores. The greatest clustering of high-factor scores occurs in the Big Meadow area and the headwaters of Bullion Canyon. Another clustering of high factor scores occurs in the Blue Lake area. It is significant to note that the streams draining the Alunite Ridge area, postulated to overlie a possible porphyry molybdenum-bearing intrusive (Cunningham and Steven, 1979b), also have high factor scores. The Grassy Creek uranium anomaly is weakly anomalous with respect to factor 4.

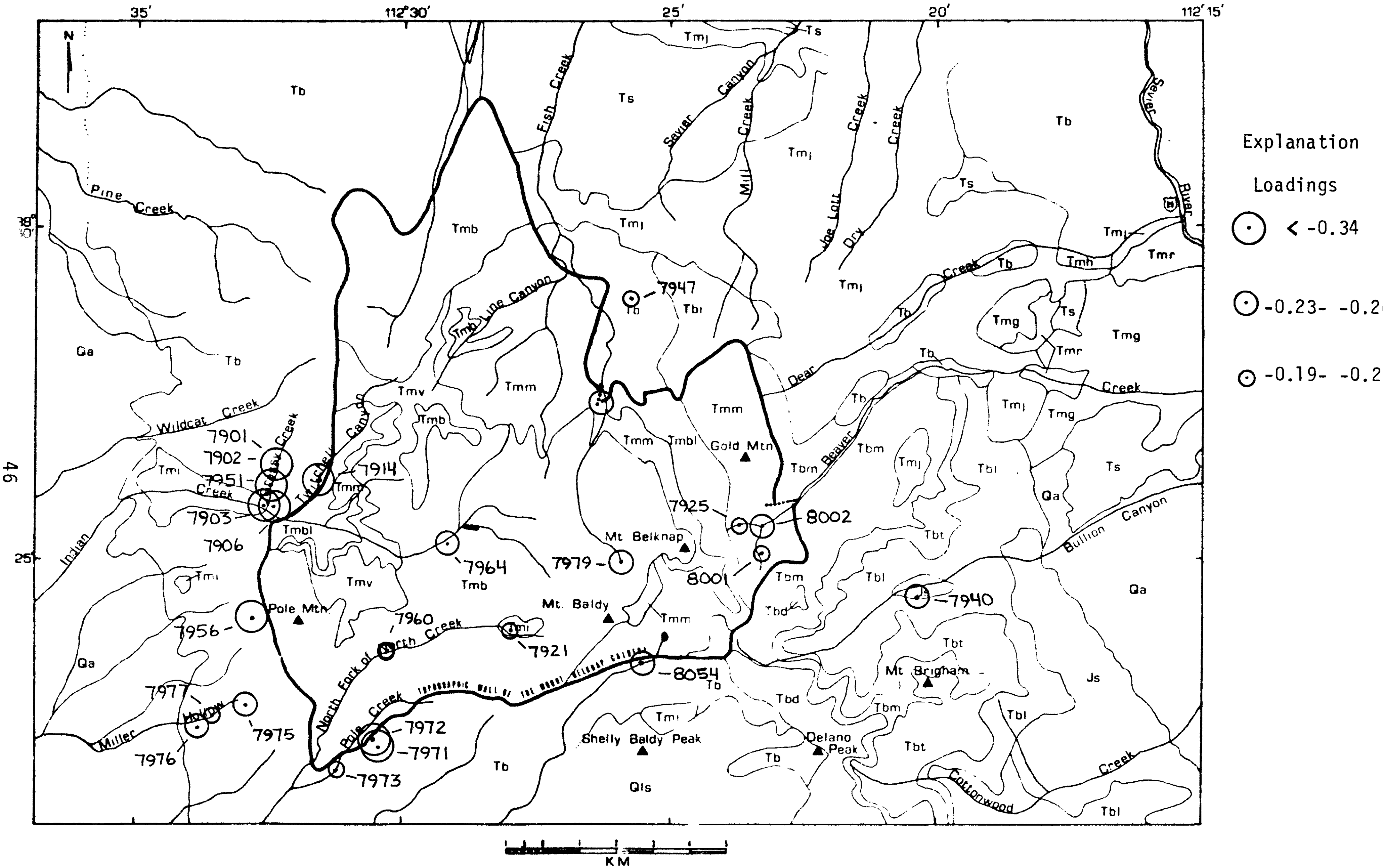

Figure 26 -- Distribution of scores for factor 3. See figure 2 for description of geologic units.

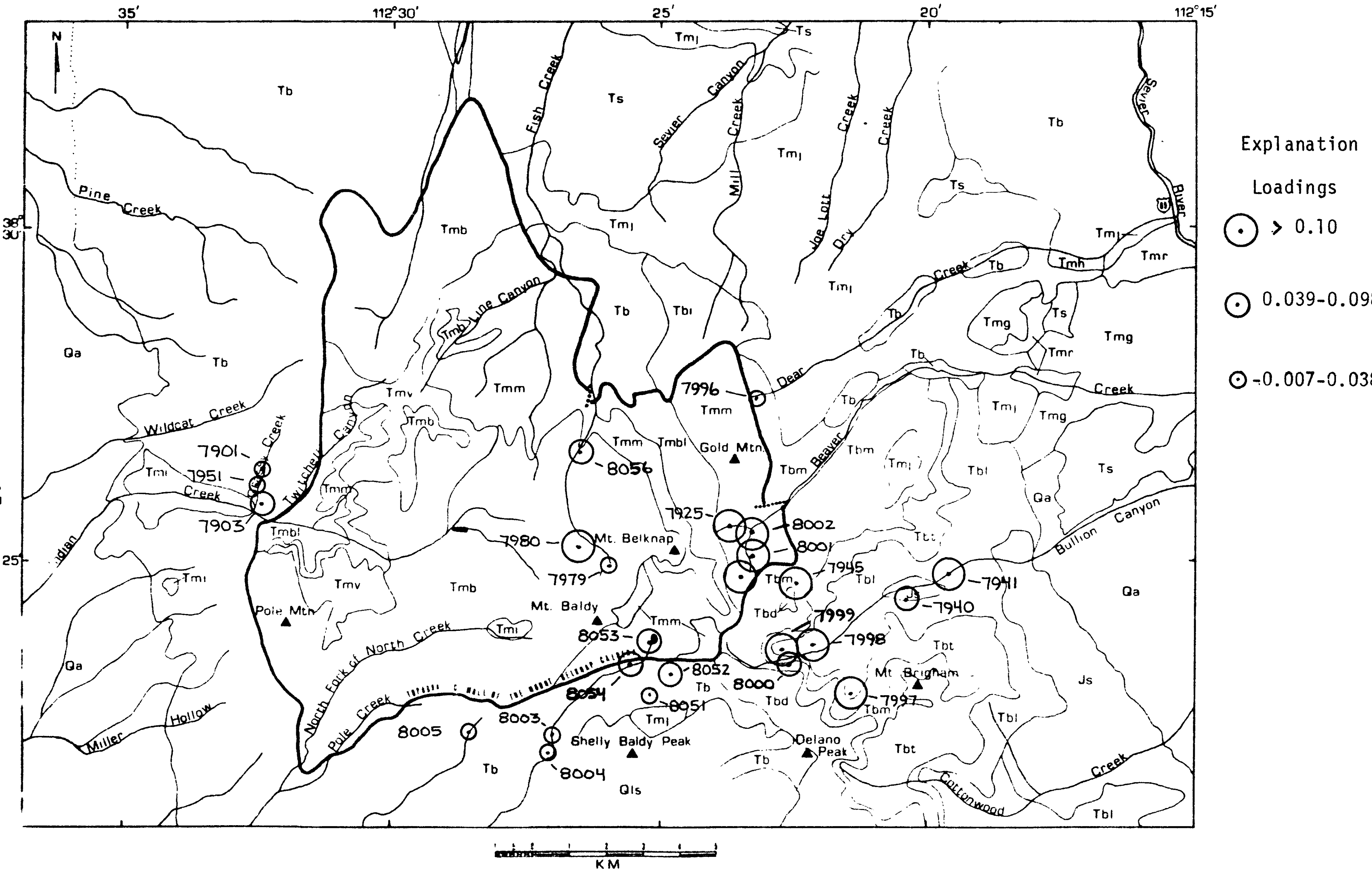

Figure 27 -- Distribution of scores for factor 4. See figure 2 for description of geologic units.

Factors 3 and 4 can be combined to depict a mineralizing sequence. The mineralizing model of Cunningham and Steven (1979b) depicts vein uranium-type mineral deposits related to intrusive implacement, which may contain deeper molybdenum bearing deposits, that occurred under Alunite Ridge. There are two other possible sites where this type of mineralizing sequence may have occurred. The Big Meadow uranium anomaly may center near what may be an intrusive extending from Big Meadow to Blue Lake. The level of erosion may have removed most of the uranium-type vein mineral deposits. There is a probability that an intrusion under the area may contain associated molybdenum mineral deposits. A second intrusive may be associated with the Grassy Creek anomaly. Molybdenum mineralization may be associated with the intrusion, possibly at a greater depth. There are no anomalous scores for factor 4 that coincide with the Pole Creek or Miller Hollow uranium anomalies. This lack of coincidence may indicate that the uranium anomalies are probably epigenetic in origin.

CONCLUSION

Water geochemistry is an extremely useful tool in exploration geochemistry. Chemical modeling and multivarient statistical analysis can be powerful tools when interpreting multispecie data, particularly in areas with complex geological and geochemical controls.

An interpretation of possible mineralized suites has been facilitated by the use of multivarient statistical analysis. Three molybdenum anomalies have been identified. The largest anomaly occurs in the Big Meadow area; (a second anomaly is associated with Alunite Ridge) and a lesser anomaly occurs in the Grassy Creek area. Four uranium anomalies have been identified, the largest being the Grassy Creek area. Other areas of interest are the Pole Creek, Miller Hollow, and Big Meadow anomalies. Using the model of Cunningham and Steven (1979b) for the Alunite Ridge area, it is postulated that the Big Meadow and Grassy Creek uranium anomalies may be associated with underlying intrusives that may contain molybdenum mineral deposits. The Miller Hollow and Pole Creek uranium anomalies are probably epigenetic in origin. Other occurrences of epigenetic uranium mineral deposits may be located within the caldera.

REFERENCES CITED

Ball, J. W., Nordstrom, D. K., and Jenne, E. A., 1980, Additional, and revised thermochemical data and computer code for WATEQ2--A computerized chemical model for trace and major element speciation and mineral equilibrai of natural waters: U.S. Geological Survey Water-Resource Investigations 78-116, 109 p.

Boyle, R. W., Hornbrook, E. H. W., Allan, R. J., Dyck, W., and Smith, A. V., 1971, Hydrogeochemical methods--Application in the Canadian Shield: Canadian Institute of Mining and Metallurgy Bulletin, v. 64, p. 60-71.

Brown, Eugene, Skougstad, M. W., and Fishman, J. J., 1970, Methods for collection and analysis of water samples for dissolved minerals and gases: U.S. Geological Survey Techniques for Water-Resource Investigations TWI 5-A1, 160 p.

Cameron, E. M., 1978, Hydrogeochemical methods for base metal exploration in the northern Canadian Shield: Journal of Geochemical Exploration, v. 10, p. 219-243.

Cunningham, C. G., and Steven, T. A., 1978a, Geologic map of the Delano Peak NW quadrangle, west-central Utah: U.S. Geological Survey Miscellaneous Field Studies Map MF-967.

_______, 1978b, Postulated model of uranium occurrence in the central mining Area, Marysvale District, west-central Utah: U.S. Geological Survey Open-File Report 78-1093, 19 p.

_______, 1979a, Geologic map of the Delano Peak NE Quadrangle, west-central Utah: U.S. Geological Survey Miscellaneous Field Studies Map MF-1105.

_______, 1979b, Geologic map of the Deer Trail Mountain-Alunite Ridge Mining Area, west-central Utah: U.S. Geological Survey Miscellaneous Geologic Investigations Map I-1230.

Cunningham, C. G., and Steven, T. A., 1979c, Environments favorable for the occurrence of uranium within the Mount Belknap caldera, Beaver Valley and Sevier River Valley, west-central Utah: U.S. Geological Survey Open-File Report 79-434, 15 p.

_______, 1979d, Mount Belknap and Red Hills calderas, and associated rocks, Marysvale volcanic field, west-central Utah: U.S. Geological Survey Bulletin 1468, 34 p.

_______, 1980, Geologic map of the Beaver NE Quadrangle, Utah: U.S. Geological Survey Miscellaneous Field Studies Map MF-1191.

Davis, J. C., 1973, Statistics and data analysis in geology: New York, John Wiley and Son, Inc., 550 p.

Fournier, R. O., and Truesdell, A. H., 1973, An empirical Na-K-Ca geothermometer for natural waters: Geochimeca et Cosmochimica Acta, v. 37, p. 1255-1275.

Klovan, J. E., and Imbrie, J., 1971, An algorithm and Fortran-IV program for large-scale Q-mode factor analysis and calculation of factor scores: Journal of the International Association of Mathematical Geology, v. 3, no. 1, p. 61-77.

McHugh, J. B., 1979, Portable field kit for determining uranium in water: U.S. Geological Survey Open-File Report 79-249, 14 p.

McNair, A. H., 1951, Paleozoic stratigraphy of northwestern Arizona: American Association of Petroleum Geologists Bulletin, v. 35, no. 3, p. 525-526.

Miller, W. R., and Ficklin, W. H., 1976, Molybdenum mineralization in the White River National Forest, 18 Colorado: U.S. Geological Survey Open-File Report 76-711, 29 p.

Miller, W. R., and Drever, J. I., 1977, Chemical weathering and related controls on surface water chemistry in the Absaroka Mountains, Wyoming: Geochimeca et Cosmochimica Acta, v. 41, p. 1693-1702.

Miller, W. R., McHugh, J. B., and Ficklin, W. H., 1979, Possible uranium mineralization, Mineral Mountains, Utah: U.S. Geological Survey Open-File Report 79-1354, 44 p.

_______, 1980, Possible uranium mineralization, Beaver Basin, Utah: U.S. Geological Survey Open-File Report 80-508, 35 p.

Orion Research, Inc., 1975, Orion Research analytical method quide, 7th ed.: Cambridge, Massachusetts.

Paces, T., 1975, Asystematic deviation from Na-K-Ca geothemometer below 75° and above 10^{-4} at PcO2: Geochimica et Cocmochimica Acta, v. 39, p. 541-544.

Perkin-Elmer Corporation, 1976, Analytical methods for atomic absorption spectrophotometry: Norwalk, Connecticut, Perkin-Elmer Corp., 586 p.

_______, 1977, Analytical methods for atomic adsorption spectrophotometry, using the HGS graphite furance: Norwalk, Connecticut, Perkin-Elmer Corp., 286 p.

Rowley, P. D., Lipman, P. W., Mehnert, H. H., Lindsey, D. A., and Anderson, J. J., 1978, Blue Ribbon lineament, an east-trending structural zone within the Pioche mineral belt of southwestern Utah and eastern Nevada: U.S. Geological Survey Journal of Research, v. 6, no. 2, p. 175-192.

Smee, B. W., and Hall, G. E. M., 1978, Analysis of fluoride, chloride, nitrate, and sulfate in natural waters, using ion chromatography: Journal of Geochemical Exploration, v. 10, no. 3, p. 245-258.

Steven, T. A., 1977, Geologic map of the Sevier SW Quadrangle, west-central Utah: U.S. Geological Survey Miscellaneous Field Studies Map MF-962.

Steven, T. A., and Cunningham, C. G., 1971a, Clinoptilolite resources in the Tughar-Mountain, west-central Utah: U.S. Geological Survey Open-File Report 79-535, 20 p.

_______, 1979b, Uranium potential of the Big John Caldera, Beaver County, Utah: U.S. Geological Survey Open-File report 79-527, 16 p.

_______, 1980a, Geologic map of the Sevier SE Quadrangle, west-central Utah: U.S. Geological Survey Miscellaneous Field Studies Map MF-1109.

_______, 1980b, Integrated uranium systems in the Marysvale volcanic field, west-central Utah: U.S. Geological Survey Open-File Report 80-524, 39 p.

Steven, T. A., Cunningham, C. G., Naeser, C. W., and Mehnert, H. H., 1978, Revised statigraphy and radiometric ages of volcanic rocks and mineral deposits in the Marysvale area, west-central Utah: U.S. Geological Survey Bulletin 1469, 40 p.

Steven, T. A., Cunningham, C. G., and Rowley, P. D., 1978, Geology and mineralization in the Marysvale mining area, west-central Utah, in Guidebook to mineral deposits of southwestern Utah: Utah Geological Association Publication 7, p. 67-70.

Tripathi, V. S., 1979, Factor analysis in geochemical exploration: Journal of Geochemical Exploration, v. 11, p. 263-275.